CHALMERS
UNIVERSITY OF TECHNOLOGY

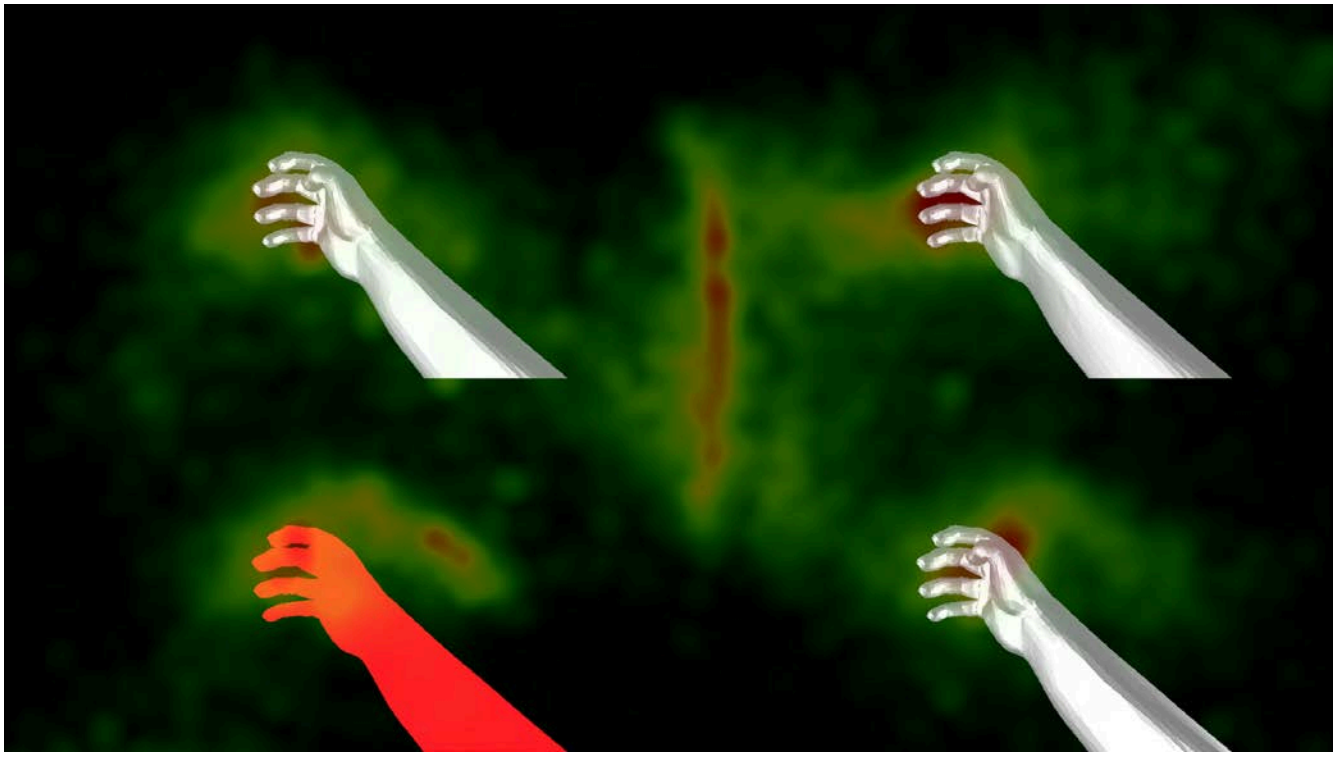

Objective Measurement of the Experience of Agency during Myoelectric Pattern Recognition based Prosthetic Limb Control using Eye-Tracking

Master's thesis in Biomedical Engineering

Tryggvi Kaspersen

Department of Electrical Engineering
Signal processing and Biomedical engineering
Biomechatronic & Neurorehabilitation Laboratory
CHALMERS UNIVERSITY OF TECHNOLOGY
Gothenburg, Sweden 2019
Master's Thesis

MASTER'S THESIS IN BIOMEDICAL ENGINEERING 2019

Objective Measurement of the Experience of Agency during Myoelectric Pattern Recognition based Prosthetic Limb Control using Eye-Tracking

Master's Thesis in Biomedical Engineering

Tryggvi Kaspersen

Department of Electrical Engineering
Signal Processing and Biomedical Engineering division
Biomechatronics & Neurorehabilitation Laboratory
CHALMERS UNIVERSITY OF TECHNOLOGY
Göteborg, Sweden 2019

Objective Measurement of the Experience of Agency during Myoelectric Pattern Recognition based Prosthetic Limb Control using Eye-Tracking

Master's Thesis in Biomedical Engineering

Tryggvi Kaspersen

Examensarbete EENX30
Institutionen för Elektroteknik
Chalmers tekniska högskola, 2019

Supervisors: Dr. Max Jair Ortiz-Catalan, Eva Lendaro, and Autumn Naber
| Department of Electrical Engineering.
Examiner: Dr. Max Jair Ortiz-Catalan
| Department of Electrical Engineering.

Department of Electrical Engineering
Signal Processing and Biomedical Engineering division
Biomechatronics & Neurorehabilitation Laboratory
Chalmers University of Technology
SE-412 96 Göteborg
Sweden
Telephone: + 46 (0)31-772 1000

Cover:
An overlay of a semi-transparent heatmap showing the distribution of all recorded eye-movement durations in the thesis experiments (for further discussion, see section: 4.1.1 Visualization of gaze data). Underlaid is a reference image of the visual stimulus presented during each trial: four virtual reality arms controlled by pattern recognition of recorded myoelectric signals with one arm in the third quadrant flashing red as occurred in the experimental reaction time task (for further discussion see: 3 Methods).

Typeset in MS Word
Göteborg, Sweden, 2019

Objective Measurement of the Experience of Agency during Myoelectric Pattern Recognition based Prosthetic Limb Control using Eye-Tracking

Master's Thesis in Biomedical Engineering

Tryggvi Kaspersen

Department of Electrical Engineering
Signal Processing and Biomedical Engineering division
Biomechatronics & Neurorehabilitation Laboratory
Chalmers University of Technology

ABSTRACT

Instilling the sense of agency (SoA) towards a prosthetic limb is essential for it to be felt like an integral part of the body, rather than just an inanimate tool. In this context, SoA can be described as an experience of voluntary control over a prosthesis through the generation of predictable outcomes in daily life activities. Being able to reliably measure this perceived experience could serve as a window into an amputee's intrinsic feeling of being in control of the actions of their artificial limb. Thereby providing valuable information that could potentially reflect the user's acceptance of the prosthetic device. In previous studies, explicit assessments of the SoA have relied on subjective self-reports that are influenced by individual interpretation or opinion which can be highly variable from person to person, instead of an objective quantitative outcome measure. Therefore, the purpose of this thesis is to evaluate the feasibility of using an eye-tracker to objectively measure the experience of agency towards a virtual limb controlled with state-of-the-art techniques used in prosthetic control. An experiment was developed and conducted on six non-disabled participants, each presented with four controllable virtual reality (VR) arms displayed on a computer monitor. Myoelectric pattern recognition for the decoding of participants' movement intentions from the electrical activity produced by forearm muscles was used as a control method for the VR arm. By using the research platform BioPatRec, it was possible to translate distinctive patterns in EMG signals due to arm muscle contractions into movement predictions, which were then executed in real-time by the VR arms. During each experimental trial, the participant's task was to detect and respond with a keypress to randomly occurring flashes of red color on a single virtual arm while simultaneously maintaining continuous movement on the VR arms. Meanwhile, two measurements took place: eye-tracking and the reaction time to an entire VR arm flashing red for a brief moment. Unbeknownst to participants and unrelated to their task, the VR arm controllability randomly varied throughout the experiment by alterations to the movement predictions, made by the control algorithm, affecting all but one VR arm. Thus, making one randomly chosen VR arm was always more controllable than the other three. The results showed that significantly more time was spent looking at the most controllable virtual arm. However, there was no indication that concurrent controllability over a VR arm influenced the reaction time to a VR arm flashing red. Given the exploratory nature of this study and the small sample size, further improvements to the proposed approach are warranted if it is intended to be used as a measurement of perceived SoA over an artificial limb controlled with MPR-based prosthetic control.

Keywords: Sense of agency, Myoelectric pattern recognition, upper limb prosthetics, the embodiment of prosthetic limbs, virtual reality representation of arms, eye-tracking, reaction time.

Acknowledgments

In this section, I decided to take the opportunity to express my gratitude towards several individuals that have helped me in the development of my thesis project.

First, I would like to thank my supervisors, Eva Lendaro & Autumn Naber, along with my examiner, Prof. Max Ortiz Catalan, for their guidance, willingness to help, and for granting me the opportunity to work on a challenging yet fascinating thesis topic. For offering her expert opinion in the field of sense of agency and valuable feedback, I would like to thank project associate professor Wen Wen at the Department of Precision Engineering at the University of Tokyo.

It has been a privilege to work alongside the great people at the Biomechatronics & Neurorehabilitation laboratory. Thanks go to all the people at the lab for the help they provided.

To all my friends I have met these past years in Gothenburg. Many thanks to my 'study group' for their warmth, camaraderie, and all the help they provided me with: Abdulrahman Alsaggaff, Alberto Nieto, Alexander Doan, Anoop Subramanian, Asta Danauskienė, Berglind Þorgeirsdóttir, Isabelle Montoya, Laura Guerrero, Mauricio Machado, Ryan Thomas Sebastian, and Wilhelm Råbergh.

I would also like to thank my friends and parents back home in Iceland for their support.

Finally, a special thanks to my girlfriend Margrét Björg Arnardóttir, for all her loving support and always being there for me.

Tryggvi Kaspersen, Gothenburg, February 2020

Contents

Abbreviations & Notations

AOI	Area of interest
CNS	Central nervous system
EMG	Electromyography
sEMG	Surface Electromyography
I-VT	Velocity threshold identification filter
MES	Myoelectric signal
MPR	Myoelectric pattern recognition
Q	Quadrant / screen-quadrant
SoA	Sense of agency
SoO	Sense of ownership
VR	Virtual reality
VRE	Virtual reality environment

1 Introduction

Loss of a limb can potentially have severe long-term consequences on a person's life. This permanently altered physical state can involve more effort to complete activities of daily life than before the amputation, as well as necessitating both behavioral and emotional adjustments. Depression, anxiety, pain at the amputation site or in the phantom limb, and inadequate adjustment towards one's replacement limb are some of the possible physical and psychological problems that are faced [1], [2].

This disabling condition is considered a global public health problem [3], [4], where nearly two hundred thousand people each year are amputated in the US alone [5]. The estimation is that the number of people living with limb loss can climb to an even higher number in the following decades, considering two of the leading causes that can lead to amputation of a limb, vascular diseases and diabetes, are similarly on the rise [5]. Therefore, there exists a demand for innovation and further development of pre-existing and new prosthetic devices for amputees.

In recent years, impressive strives have been made in the field of prosthetics to create prosthetic devices that offer increased functionality through intuitive prosthetic control based on decoding motor intent from electromyography (EMG) or myoelectric signals, and by providing tactile sensory feedback through neurostimulation [6], [7]. Despite these advancements, a considerable amount of cognitive workload and visual attention is required on behalf of the user to manipulate an artificial limb. Visual feedback is heavily relied upon in the execution of simple prosthesis manipulation tasks, where grasp critical areas of physical objects and the prosthesis itself gain a substantial amount of visual attention [8], [9]. Moreover, a natural limb greatly differs from an artificial one, the latter usually by having fewer degrees of control, by lacking an intricate in-built sensory system, by having different appearance and mass, and by being more difficult to control.

By developing new prosthetic devices with the ambition of closing the gap between artificial and natural limbs, we move closer to the ideal of integrating the artificial limb with the user's body, and away from it being experienced and used as an inanimate supplemental tool. As this pursuit leads to improved usability of prosthetic control systems, the amputees should feel like they are in control of the actions performed with the artificial limb, i.e., have a sense of agency (SoA) over it. Providing amputees with strong agentic experience over a prosthesis is thought to be linked to the embodiment of the replacement limb as an integral part of the body [10], [11]. Therefore, instilling SoA over the artificial limb serves as a step closer

towards the ultimate goal of developing a prosthesis that is ‘experientially transparent’ in the same manner as the biological limb that it is meant to replace.

In a recent methodological framework article by Schofield *et al.* [12], an SoA assessment protocol over a neural-machine interface control of virtual prosthetic hands was described. By implementing this method, the perceived SoA towards the prosthetic control can be characterized through previously researched explicit and implicit means (i.e., psychophysical questionnaire and time interval estimation between a voluntary action and effect, respectively). However, both measures rely on the participant’s self-reports that are based on individual experience or awareness and can potentially produce a highly variable inter-participant result.

To the best of our knowledge, no prior studies have attempted to objectively assess perceived SoA over myoelectric pattern recognition (MPR) control-based virtual terminal device by tracking the controller’s allocation of visual attention during use. Earlier studies on visual search have indicated that visual attention is attracted to self-generated motion which is displayed on a visual stimulus that elicits a strong SoA [13], [14]. As an example of such a stimulus, an abstract shape or a virtual avatar is shown on a monitor, which is congruent with the subject’s voluntary movements during motion tracking or moving a computer mouse. While simultaneously moving multiple external objects, a single ‘self’-stimulus appears to stand out visually among several other distracting stimuli of identical appearance, for which motion is either partially or entirely incongruent with the participant’s intended movements. This visual salience has been reflected by faster self-recognition when actively moving the stimulus compared to when it is moved by someone else and is thought to be augmented by the SoA experienced as a consequence of voluntarily moving the stimulus.

Inspired by the aforementioned paradigm, this project aims to examine SoA by translating self-produced motion to virtual limbs using state-of-the-art prosthetic control techniques, as illustrated in Figure 1. The hope is to lay the groundwork of an assessment procedure of perceived SoA towards different control algorithms driving the prosthetic-limb control systems and gaining. In doing so, a valuable insight might be gained into how well amputees feel they have voluntary control over the actions produced with a prosthetic limb. Eventually, this method could guide the development of prosthetic treatments and contribute to the goal of restoring an amputee’s loss of functionality and promote prosthetic acceptance.

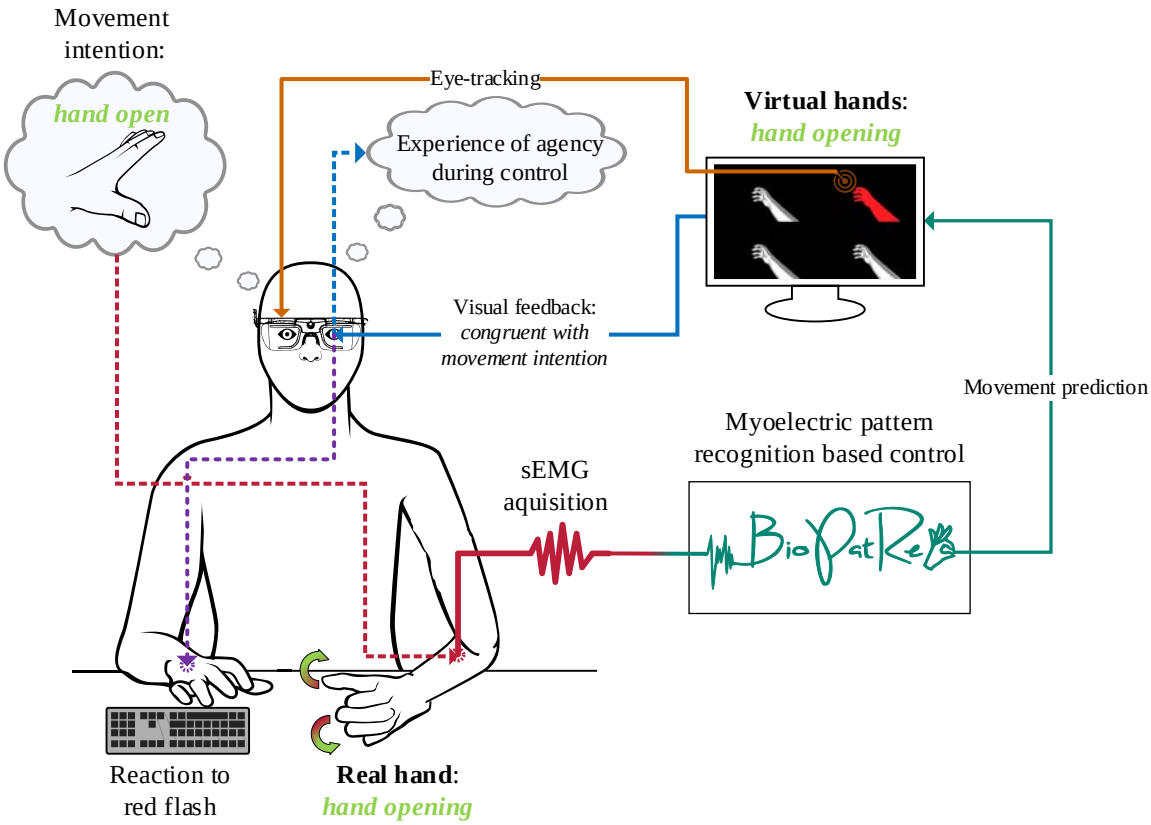

Figure 1. A graphical representation of the process of experiencing agency over a virtual prosthesis controlled via myoelectric pattern recognition (MPR) based prosthetic limb control interface. The eye-tracking glasses worn by the participant further encapsulates the objective of the thesis: assess the feasibility of objectively measuring agency in the context of real-time MPR-based control over a virtual reality arm by recording the subject's simultaneous eye-movements on the displayed arm. Figure adapted by [15].

The goal is to study the feasibility of using eye-tracking as an objective and quantitative measure of sense of agency during MPR prosthesis control. Examination of the experience of agency in the context of MPR-based control over virtual upper limbs with non-disabled participants is the extent to which the thesis' scope will be limited. An experiment was developed (see Figure 1), which involved a simple detection task for the participants while they simultaneously interacted with four displayed VR arms via MPR-interface, with each VR arm having varying degrees of controllability. Meanwhile, the participant's eye-movements were recorded. It was hypothesized that the participant's visual attention would be preferentially focused on the VR arm, which provided the highest level of controllability. Based on that hypothesis, it was expected that by devoting a significant amount of attention towards a high level of control over a VR arm, less time would be taken to react, by a keypress, to the same VR arm flashing a red color for a brief moment, as seen on Cover figure and Figure 1.

1.1 Thesis outline

Chapter 1 – Introduction

- A general discussion on the objective and aims of the thesis.

Chapter 2 – Background

- Necessary background information provided for a greater understanding of the core concepts studied and used in the thesis, e.g.:
    - Sense of agency as an essential factor for the embodiment of prosthetic devices, theories on the emergence of agency, measurements of the experience of agency, myoelectric-based prosthesis control, ending with a brief discussion on eye-tracking.

Chapter 3 – Methods

- Description of the designed methodology used in the study, along with the explanation of the experimental setup, features of the myoelectric-based virtual reality arm control, experimental design, and data analysis.

Chapter 4 – Results

- The resulting eye-tracking and reaction time dataset from experiments conducted by six non-disabled participants are presented and analyzed.

Chapter 5 – Discussion

- The findings of the study are discussed and summarized, along with proposed improvements to the implemented approach for future studies.

2 Background

When an amputee has substituted a limb with a prosthetic device, it is evident that the wearer recognizes the bodily attachment differently from their original extremity. If the latter was unimpaired, it was not only tightly interwoven with their body's intricate sensorimotor system but highly capable of carrying out one's intended movements. As a consequence, the amputee might perceive a weaker possessive experience towards the replacement limb, or failure to recognize it as a part of one's self, and experience a decreased dexterity using the prosthesis compared to the original extremity. The view is that these two experiences, known as the sense of ownership (SoO) and sense of agency (SoA), respectively, guide our cognitive processes for us to become aware of the differences between what constitutes as being a part of the self and what does not [16], [17]. Consequently, the idea is that these experiences contribute to the embodiment of extracorporeal structures [18], [19]. De Vignemont [11] posits that the embodiment of objects, like a prosthetic limb, only occurs if the processing of its properties is in the same manner as the properties of one's own body.

2.1 Sense of Agency (SoA)

In the literature, the standard description of the phenomenon of sense of agency refers to the perceived notion of being an instigator of action and causing the subsequent outcome of that action. This is often described as the "sense that I am the one who is causing or generating an action" [16] and only differs from the sense of ownership in a situation when conducting an involuntary action. We might still consider ourselves the owners of an action or a movement even though it is unintentional. However, the same does not necessarily apply for our agentic experience towards that uncontrolled action. During a reflex examination at the hospital, we might not consider ourselves causing the reflexive movement of our leg when the hammer hits our knee. We are aware that the doctor is responsible for the said movement, but experience our own body moving, and therefore, the movement garners a sense of ownership.

The following section contains an overview of the most prominent theories about the processes leading up to the emergence of SoA and how most researchers go about measuring this experience. The theories demonstrate by which mechanism SoA is thought to arise towards an event, and which various influencing factors are believed to be involved in the formation of an overall SoA estimation. Therefore, a theoretical background exists for studying SoA, which

can steer the design of a paradigm aimed at bringing out this experience and for testing out a hypothesis relating to SoA.

2.1.1 Theories

2.1.1.1 The comparator model

The occurrence of the experience of agency, as in that reflex examination example mentioned above, is generalized over other situations by implementing the often-cited comparator model [19]–[21]. This theory focuses primarily on explanations of motor control. However, it is frequently also used as an explanation of how SoA arises and as a foundation in other theories on SoA [22]. A comparison of information generated during the series of cognitive processes leading to and after the execution of a movement forms the basis of the model, see Figure 2. Contrasting the motor intention of the actor, the resulting reafferent sensory feedback in response to the movement, and the predicted state of the motor system based on the information before the execution of the movement [23].

The chain of events starts with the formation of an action intention, which then registers as a cortical response in the motor cortex. From the central nervous system (CNS), efferent nerves conduct neuroelectric signals to the appropriate muscle for the execution of the intended movement. Subsequently, the individual experiences a sensory outcome as a consequence of the altered state of the body, e.g., raising a limb. The sensory feedback can be proprioceptive, raised position of the extremity relative to the whole body, and visual, the sight of the arm moving. In conjunction with the intentional movement, a copy of the motor command is generated as a reference (called the ‘efference copy’) and compared with the real sensory information (reafferent) generated as a result of the movement, and the initially desired state. If there is a match between these signals, a sense of agency arises, or alternatively the lack of it in the case of a mismatch. Conscious awareness of the SoA is not present until there is a mismatch during the comparison [20]. Furthermore, this model describes in a way our inbuilt self-recognition mechanism. Allowing us to readily identify our own actions among other people in an ambiguous situation, e.g., looking at ourselves in a live security camera feed on a grocery store TV. This discrimination is facilitated by us experiencing SoA following an intentional action and not towards the actions of others [13].

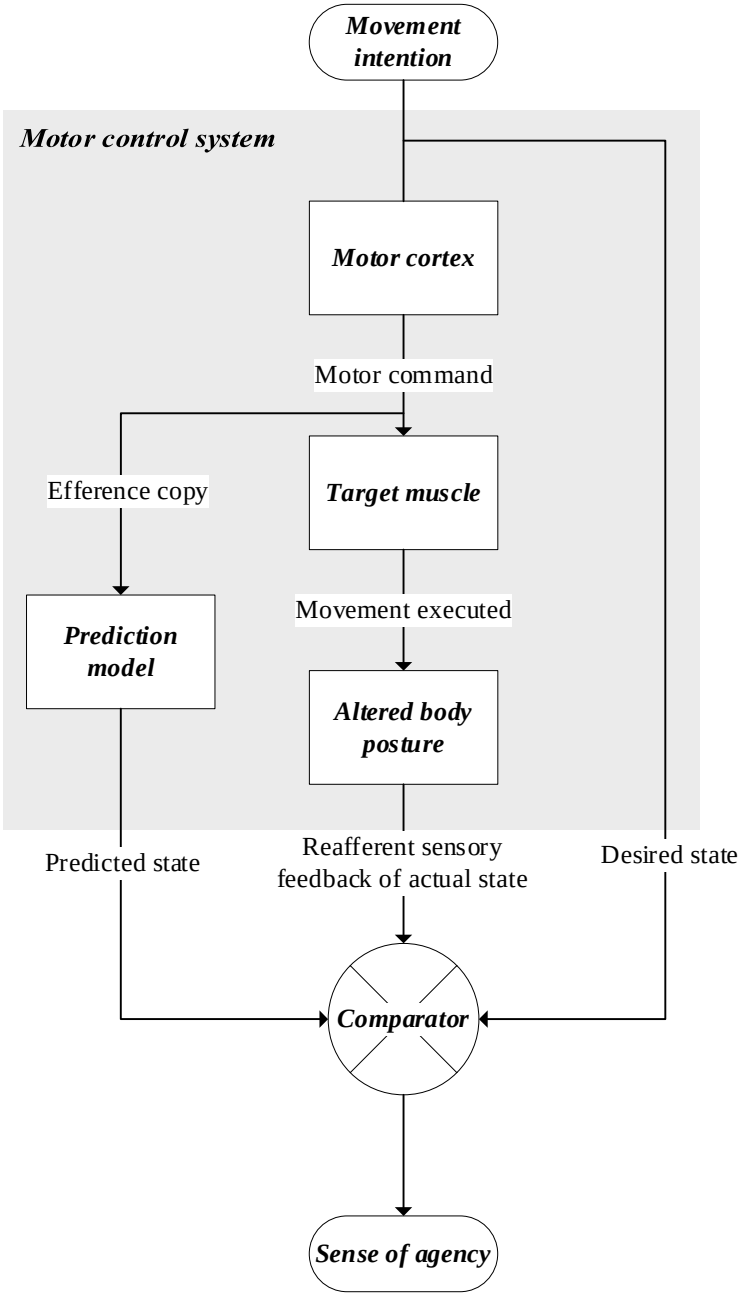

Figure 2. A customized diagram of the comparator model representing the relevant sensorimotor processes involved in generating a sense of agency towards a movement, adapted by [19], [23].

2.1.1.2 The multifactorial weighting model

New theories followed in the footsteps of the comparator model, with the focus on expanding the framework beyond motoric signal processing by including other factors that seem to influence the SoA. One such view was held by Synofzik *et al.* [22], suggesting a breakdown of the concept into the feeling and judgment of SoA. The former aspect is more related to a low-level feeling of being an agent of an action, being dependent on authorship cues such as

proprioception and reafferent sensory feedback of movements. However, the judgment of agency relates more to top-down processes impacting agency formation, i.e., social context, beliefs, and thoughts. The extent to which either judgment or feeling of agency contributes to the overall SoA estimation depends on the importance or weight of top-down or bottom-up information in any given situation. Thus, the overall agency estimation hinges on the collaborative involvement of these two subcategories of SoA, see Figure 3.

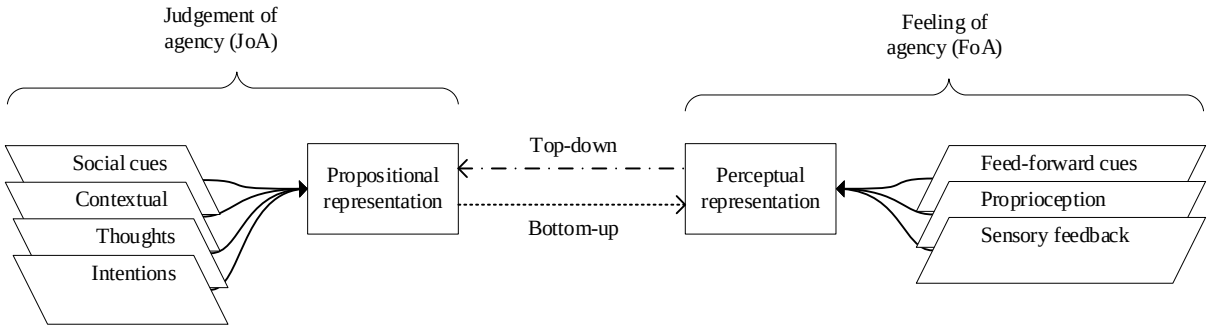

Figure 3. A diagram of the multifactorial two-step account of agency, showing the breakdown of SoA into judgment and feeling of agency. Both factors, depend on authorship cues (represented by parallelograms) relating to either sensorimotor events (FoA) or conceptual cues (JoA) to form an overall SoA [22].

2.1.1.3 The cue integration account

Another view suggests that SoA is formed by implementing internal statistical models that integrate all available sensory sources of information, based on their reliability in each situation, for the formation of a SoA estimation [24]. Furthermore, this model can also implement Bayes's rule to incorporate the agent's prior information or top-down influences to augment the reliability of the SoA estimation even further, e.g., intent, belief, or situationally based expectations preceding the action. By implementing the maximum likelihood estimation approach, this cue integration account of SoA ensures that an SoA estimation is more robust when it consists of multiple sources of information compared to an overall estimation based on a single cue. Each available agency cue provides an individual with information about the agentic origin of an action based on specific uncertainty. Therefore, a more accurate agency estimation is generated by accumulating multiple agency cues together. To illustrate this point, you could be seated alone in a room when your arm uncontrollably moves a bit. Considering only sensorimotor cues for the agency estimation of your sudden arm movement, it would not be enough to create an accurate agentic estimation. Incorporating external cues such as the prior

information might be a more reliable source. Therefore, the knowledge of you being the only person in the room with the door locked might engender an SoA over the arm movement compared to motoric signals.

2.1.1.4 Theory of apparent mental causation

Both the multifactorial model and the cue integration approach, mentioned above, highlight the importance of considering situational, interpretive, and social information other than the comparator model's discrepancy detection between efferent and reafferent signals. Wegner and Wheatly [25] emphasized the role of these types of agency cues in the theory of apparent mental causation. They suggest that the extent of the experience of willing an action stems from the conditional relationship between an intention and an action: "The thought should occur before the action, be consistent with the action, and not be accompanied by other potential causes.". This theory introduces a causal pathway of SoA that undoubtedly sidelines the supposed contribution of the motor system, while also proposing that the actual cause of the action and the thought preceding it are generated through separate unconscious mental processes. The perception of the apparent path between the though and the action gives a SoA over the action.

Prior investigations have observed the importance of relying on external cues in the formation of the SoA when sensorimotor information is less accurate. Wen *et al*. [26], [27] observed the contributing impact of external cues in the formation of participant's SoA over a controllable screen-based object when steered towards solving a simple goal-oriented task. By facilitating task performance, unbeknownst to the participants, the observation was that performance-based inferences took precedence over internal efference-reafference congruency in SoA formation when the sensorimotor information source was less reliable due to added delay to the participant's intended movement of the touchpad-controlled shape. In cases when the delay in response to the object was the greatest, the participants rated their SoA being stronger despite being assisted in completing their task, which entailed reducing the control during task execution.

2.1.2 Measures of SoA

SoA does not consist of an observable quantity to be readily measured, providing researchers with the challenging task of finding a way to explore this phenomenon in a controlled environment. Many of their efforts to study SoA consist of designing an experiment that provides voluntary motion control over an external object (e.g., visual stimulus on a screen).

Additionally, the implementation of modifications to sensory feedback received as a consequence of moving the object, e.g., varying the degree of control [20]. Dependent on the implemented approach, the methods of assessing SoA can be broadly described as being explicit or implicit, a frequently used categorization in review literature [19]–[21] and prior studies [28], [29]. The interpretive side of SoA, i.e., judgement of agency, is thought to be observed when explicitly examining SoA, while implicit methods allow for the assessment of the low-level feeling of agency [22], see also Section 2.1.1.2.

2.1.2.1 Explicit measures

By directly asking the subjects about their perceived SoA, the experimenter uses subjective self-reports as an explicit outcome measure of the experience, often relying on rating scales and questionnaires. As an example, Argelaguet *et al*. [30] studied the sense of embodiment, including the sense of agency, towards three different types of controllable virtual hand representations. After solving two tasks in a virtual reality environment (VRE) by using each of the motion-capture controlled hands, participants rated their perceived SoA on a seven-point scale by answering a questionnaire, e.g..: "I felt as if the virtual representation of the hand moved just like I wanted it to, as if it was obeying my will.". The results indicated stronger SoA attributed to the less realistic hand representation among the three, due to the fact that its movements matched better with participant's real-time movements compared to that of the realistic hand representation.

2.1.2.2 Implicit measures

On the other hand, implicit assessments of SoA are determined by studying variables that are assumed to correlate with voluntary movements in an experimental setting (e.g., neuronal or behavioural). The intentional binding effect being among one of the most frequently used implicit measures [31]. Discovered by Haggard *et al*. back in 2002 [32], a stable pattern of response was observed when participants estimated the duration of a time interval, between pressing a button and subsequent auditory tone onset, as being shorter than it was when voluntarily pressing the button. However, the opposite pattern occurred when an involuntary press of a button (muscle twitch through transcranial magnetic stimulation) was produced, followed by an audible tone. Namely, the participants perceived the time interval between their involuntary action and subsequent auditory outcome as being longer than it was. As a consequence, perceived temporal compression occurring between the participant's intended

action and the following outcome was considered to be an implicit marker of SoA and labelled as the intentional binding effect, see Figure 4.

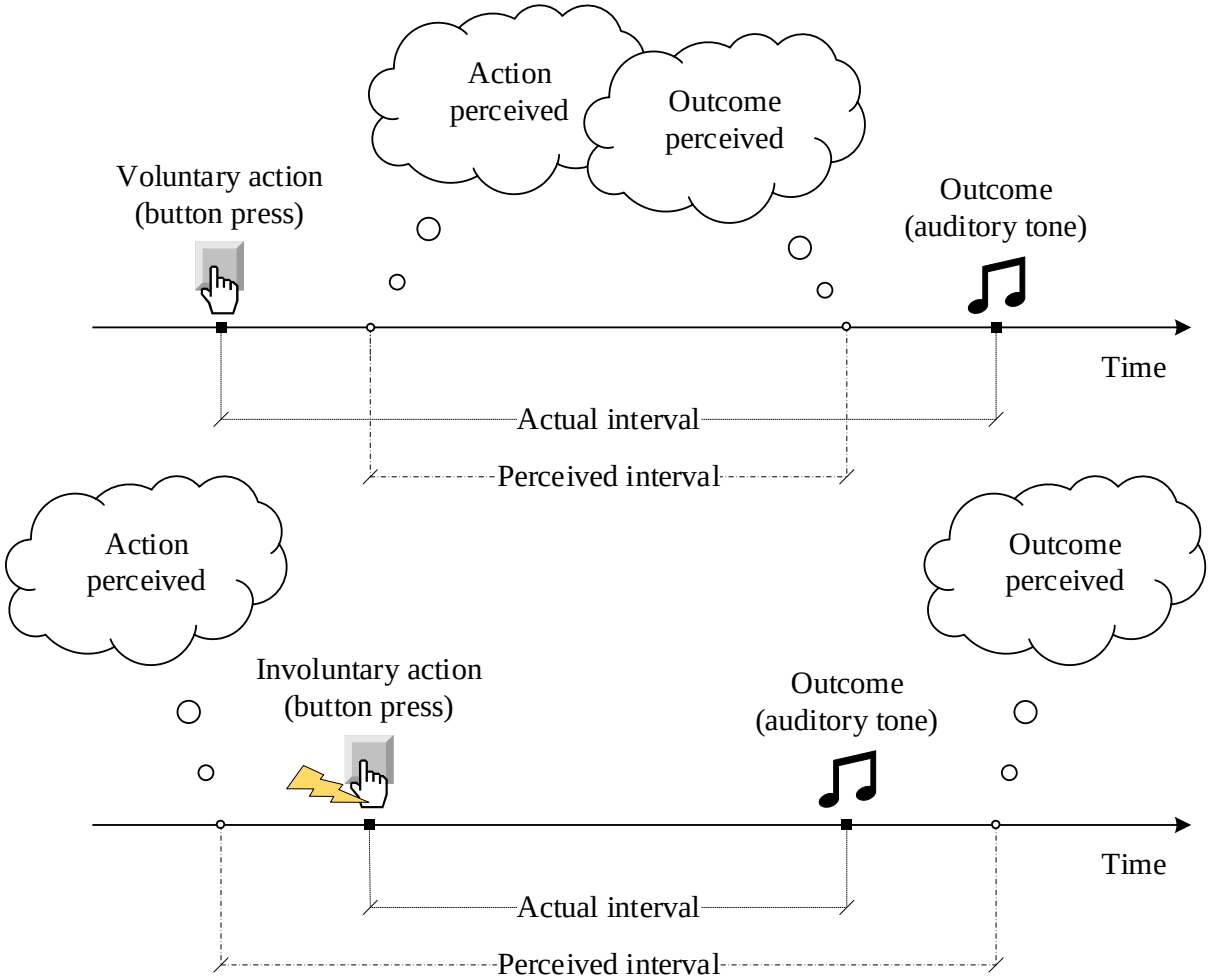

Figure 4. An illustration of the intentional binding effect occurring in a condition (top) where an auditory stimulus follows an intentional button press after a fixed amount of time. Typical observations using this paradigm indicate that participant's time estimation of the interval between a voluntary action and its sensory outcome is perceived as being shorter than it is; the reverse is true for an involuntary action-outcome condition (bottom).

Cortical response studies have observed that activity in specific brain regions correlates with voluntary action. Blakemore *et al.* [33] used magnetic resonance imaging (MRI) to monitor activity in the sensorimotor cortex of subjects when being tactilely stimulated on the surface of the palm, i.e., light contact of a piece of foam using a tactile stimulus device. The device allowed for the stimulation to be performed by either the subject or the experimenter. Results indicated heightened neuronal activity in the somatosensory cortex during an externally induced tactile response to the subject's hand compared to a self-produced one. In other words, self-induced tactile sensations appeared attenuated compared to externally induced stimulations. Thus, sensory attenuation of voluntary action consequences has been considered

as an indirect marker of SoA. Numerous studies have reported reduced auditory-related brain-activity to self-caused auditory tones compared to externally produced ones [34], see Figure 5.

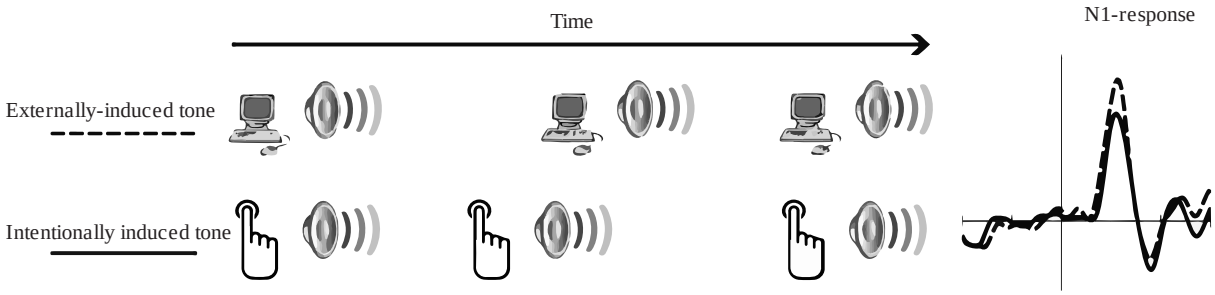

Figure 5. An example of an auditory sensory-attenuation paradigm. One condition (top), consists of random onsets of the auditory stimulus, while in the second condition (bottom), participants voluntarily produce the tone-onset by a push of a button throughout the trial. A common finding is a decreased amplitude (right) in auditory evoked potential on an electroencephalogram (EEG) in response to voluntary-triggered tones compared to externally generated ones, adapted by [34].

2.2 Myoelectric prosthetic-limb control

Since the latter part of the last century, there has been a steady development of powered prosthetic limbs that rely on myoelectric signals (MES) as an input signal for actuation [7]. The myoelectric prosthetic control scheme entails the procurement of information about the user's motor volition through MES acquisition of voluntary muscle contractions. The most commonly used MES-recording method is by either surface electrodes or implantation of electrodes closer to the muscle tissue through invasive surgery. Skeletal muscles in the vicinity of the amputation site serve as an input signal source for the prosthetic control system, considering that these types of muscles are innervated by nerves from the somatic nervous system and are involved in producing voluntary limb movements [35]. As an example and depending on the length of the residual limb, the remnants of the extensor carpi ulnaris muscle could be applied as a control site for wrist extension and hand adduction of a myoelectric prosthesis, since that muscle is active during those voluntary movements [36].

2.2.1 Pattern recognition

A popular myoelectric prosthesis control strategy, based on pattern recognition (MPR), implements machine learning algorithms for motor intention prediction by recognizing consistent patterns in continuously recorded EMG signal input [37], [38]. The control scheme uses a supervised classifier algorithm, meaning that the algorithm makes all its predictions

based on the training received using a dataset of all movements to be classified [7]. A commonality in the signal processing pipeline of MPR control methods is that they start with the acquisition of EMG signals, followed by signal pre-processing to reduce the noise present in the EMG signal, and then segmentation of the input signal to obtain muscle contraction-specific information. After that, reduction of the data dimensionality is performed by extracting signal features, thus, transforming the data into a discretized form of statistical descriptors, e.g., mean absolute value, zero crossings, slope sign changes, and waveform length [39]. Lastly, the previously trained classifier algorithm generates a movement prediction, which then outputs a movement classification for the actuation of a prosthesis. A diagram in Figure 6 illustrates the conventional signal processing pipeline of MPR-based prosthetic limb control.

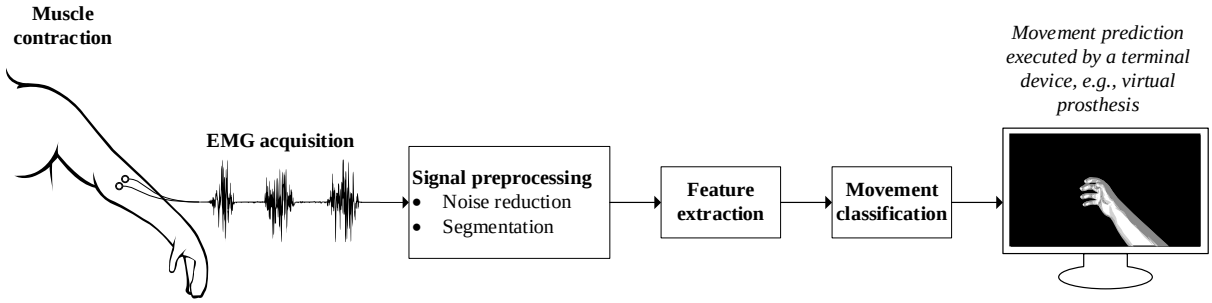

Figure 6. Diagram demonstrating the key-steps in myoelectric pattern recognition control scheme. A training session ensures that the supervised classifier algorithm recognizes EMG-patterns for real-time movement prediction. The overall signal-processing pipeline consists of the classifier algorithm receiving signal features from the preprocessed EMG signal. Subsequently, each movement prediction is then transferred and executed by the artificial limb. Adapted by [7].

2.3 Tracking eye-movements

As mentioned earlier in the introduction chapter, there appears to be a lack of any prior attempts made to implement eye-tracking based measures as an objective or implicit assessment of perceived sense of agency during MPR-based virtual prosthesis control. Prior studies suggest enhanced visual processing of external objects when self-generated motion is displayed on them, compared to presenting motion which is externally caused. Results indicate attentional capture and increased cortical activity associated with visual attention towards the self-controlled object [13], [40]. Based on the evidence and the chosen outcome measure for this study, a brief overview of eye-tracking related topics will be provided in this section.

The visual system (see Figure 7) is responsible for providing humans with the visual perception of light with a wavelength of 400 nm to 700 nm [41]. Initially, the light transmits

through the highly transparent cornea, and then passes through an aperture of the light-sensitive iris, called the pupil. After going through each of these refractive surfaces, the lens of the eye changes its shape by a process called accommodation to focus the light on the thin tissue layer known as the retina, situated in the back of the eyeball. We ultimately extract visual information from our surroundings due to the incident light, which is transduced into neural signals by photoreceptors residing on the retina. Lastly, the neuronal signals produced by the photoreceptor travel by the optic nerve to the CNS for further processing, followed by eventual visual perception of the surroundings.

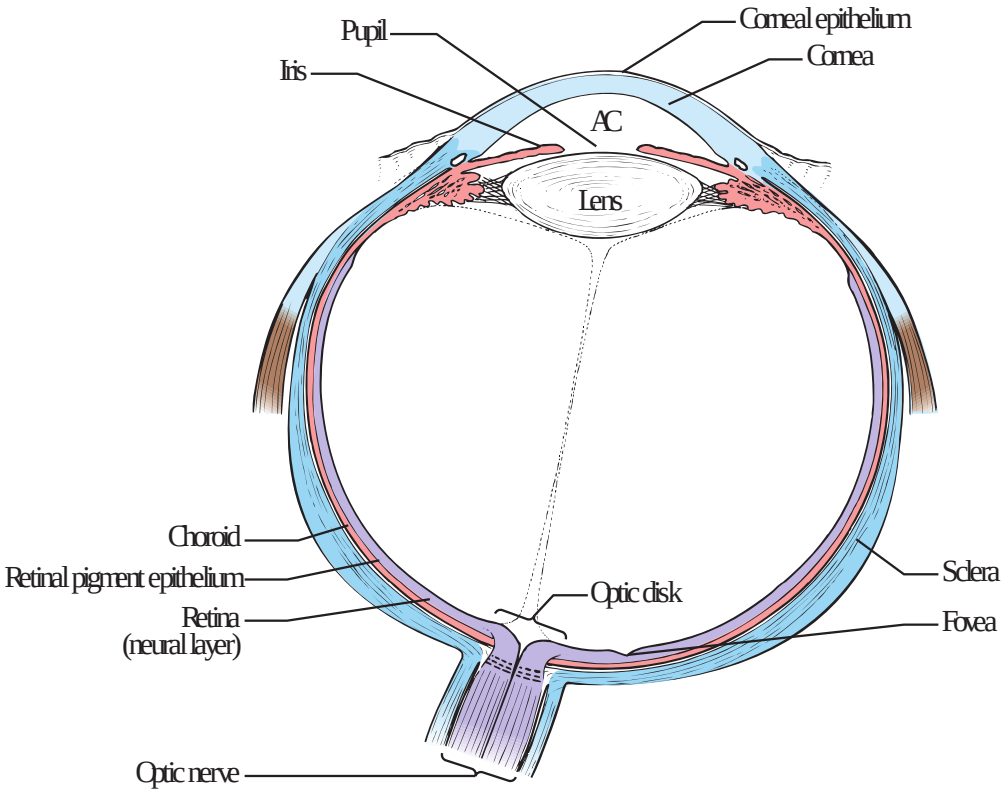

Figure 7. An illustration of a horizontal section of the anatomy of the eye, including some of its components (AC: anterior chamber) [42].

Two of the most researched eye-movements are eye-fixations and saccades. The former type consists of several miniature eye-movements which stabilize the retina over the object of interest, in order for us to extract visual information from the environment. A fixation usually lasts longer than 100 ms. Saccades are rapid movements of both eyes in the same direction in order to shift the gaze to another object of interest. During the relatively short period of a saccade, from 10 to 100ms, our vision is suppressed [42]–[44]. A typical way to graphically represent gaze data from these movements is on a gaze-plot, as can be seen in Figure 8.

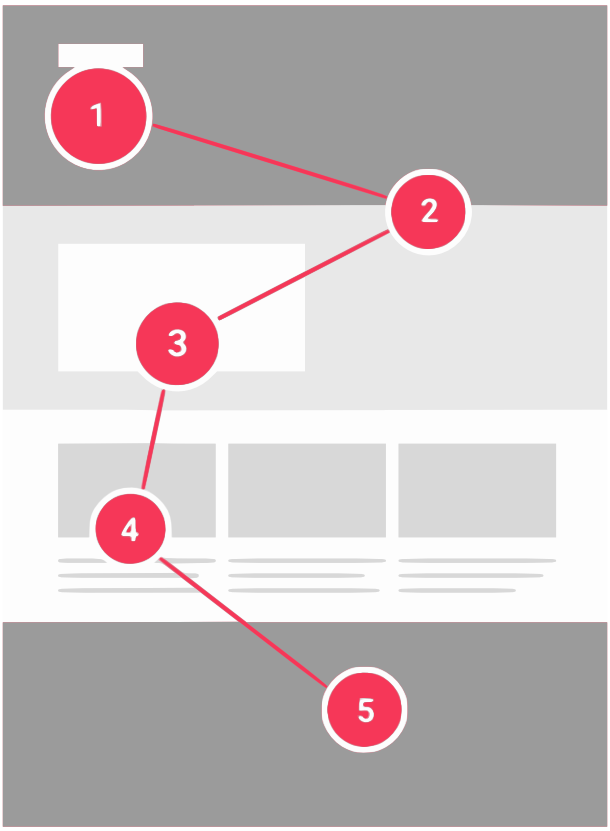

Figure 8. Gaze plot superimposed on top of a visual stimulus. A sequence of fixations intermitted by saccades, represented by a circle (duration proportional to its radius) and a connected line, respectively [45].

The Pupil Center Corneal Reflection (PCCR) is an eye-tracking method that has been frequently used for tracking these types of eye-movements. Usually, it consists of illuminating the eye using a non-distracting infrared light source to produce an apparent light reflection on the cornea, better known as a glint, and on the pupil. The eye-tracking cameras are pointed towards the eye during illumination, and a vector can be drawn between the two ocular features captured in the video to calculate the gaze direction and position, see Figure 9 for a graphical representation of PCCR [43], [46]. If the tracker's illuminator is placed close to the optical axis of the tracker's eye monitoring cameras, the pupil becomes brighter relative to the iris, also known as the bright pupil effect. However, if the illuminator is placed away from the optical axis, a darker pupil compared to the iris is captured by the tracker's eye-movement cameras.

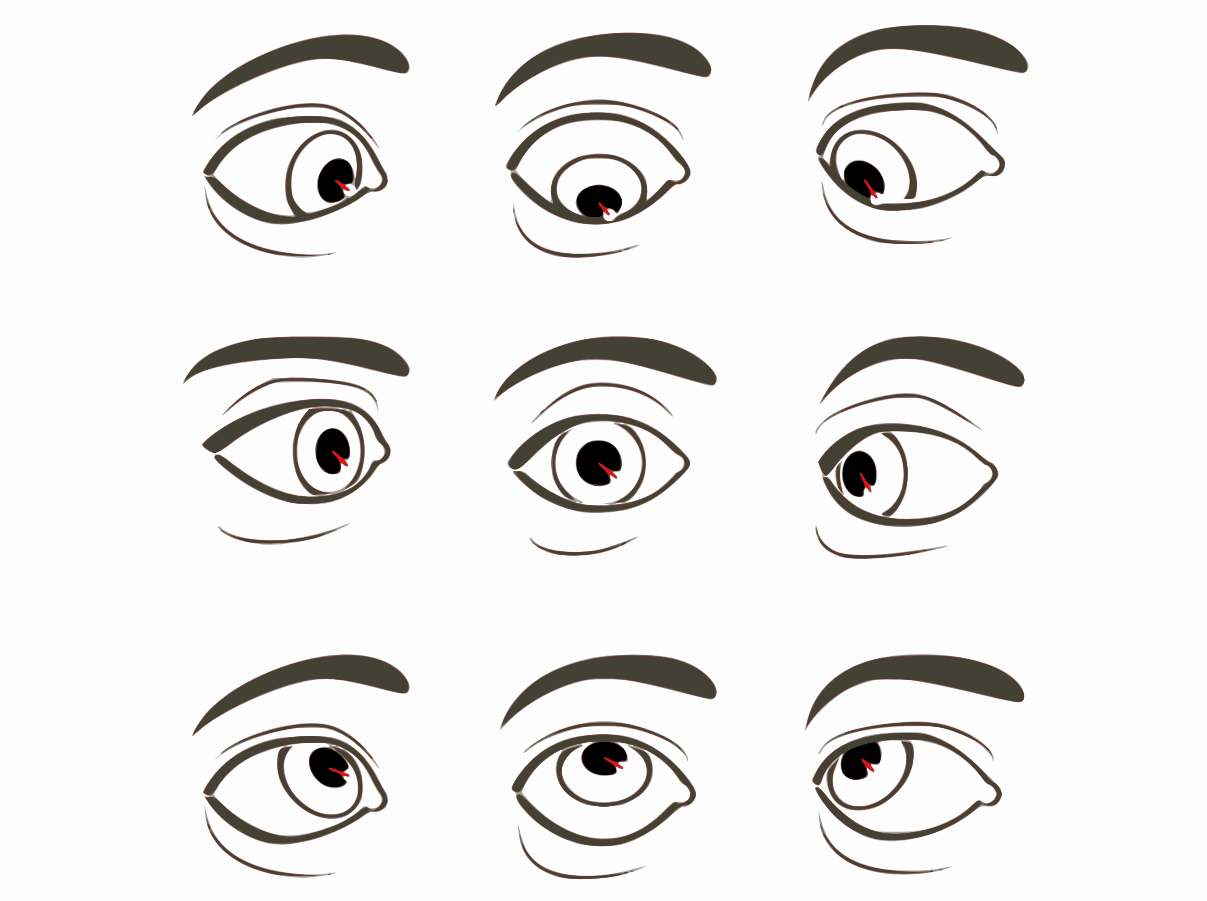

Figure 9. An illustration of the PCCR method, showing the calculated vector (in red) between the glint and the pupil reflection, relative to the eye-cameras view [47].

3 Methods

Preliminary tests were conducted on two participants to verify the feasibility of the initial experimental design and to observe whether different amounts of interference added to a myoelectric control system of four virtual arms would influence the users' attentional allocation towards the virtual terminal device. Namely, it was of interest to examine if subjects spent the most time looking at a VR arm that they had the highest level of control over. A supplementary examination to the one mentioned above was to examine whether a high level of control over a VR arm was associated with less time reacting, by a keypress, to the same VR arm flashing a red color for a brief moment (as seen on the Cover figure). Thereby, testing the thesis' hypothesis laid out in the Introduction. Results gathered from the preliminary test indicated that there was no difference between time spent looking at VR arms with various levels of controllability, as well as the reaction time to brief change to their color.

Based on these results, alterations were made and used in the final version of the experimental design which is described in detail in the following sections. The changes included: a more balanced design with equal amounts of noise conditions and red flash onsets on VR arms across all possible noise levels, making the movement speed of the VR arm twice as fast, and utilizing movements better discernable by the classifiers. To improve the appropriate gaze data capture, a smaller monitor to display the VR arms was used to ensure that all the displayed VR arms were in view of the eye-tracking glasses and to compensate for data loss due to the subject's unintentional head movements. Furthermore, the task instructions were modified to motivate the participant to carry out continuous movement of the virtual arms throughout each trial. Lastly, to ensure that each participant could manipulate all the available movements of the VR arms, practice trials were repeated as often as necessary instead of having a fixed number of trials.

Participants

Six non-disabled participants (3M/3F) were recruited based on convenience sampling, ranging in age from 23 – 32 years (mean = 26.8 & SD = 3.1). All the participants claimed to be right-handed with the mean score of 62.3 (range: 47 – 72 & SD = 10.4) on the revised version of the Waterloo Handedness scale [48], which suggested a strong preference towards using their right hand. All participants had normal or corrected-to-normal visual acuity and normal neurocognitive function of the visual and motor systems. Questionnaire response established that no participant had been diagnosed with eye-disorders (i.e., lazy eye, strabismus or

nystagmus), undergone eye-surgeries (i.e., LASIK or radial keratotomy), and wore eyeglasses with a power of more than one. Therefore, all participants met the inclusion criteria of the experiment, formed to ensure that the eye-tracking recording was of good quality. All participants gave written informed consent before participating in the experiment, which took place at the Biomechatronics and Neurorehabilitation (BNL) laboratory at Chalmers University.

Experimental setup design

A wearable eye-tracking system was used for recording gaze-data during the experimental trials as the subjects controlled on-screen virtual limbs (Tobii Pro Glasses 2 [49], Tobii AB, Danderyd, Stockholm, Sweden), see Figure 10. The eye-tracker consists of a head and recorder unit, where wireless real-time eye-tracking observation via a tablet is possible along with audio and video recording capabilities of the scene. Accelerometer and gyroscope are included in the unit to differentiate between the eye and head movements. Gaze data were recorded with a sampling rate of 50 Hz along with a front camera video recording at 25 frames per second with a 1080p resolution.

Figure 10. The wearable eye tracker used in the study (Tobii Pro Glasses 2) which includes a front-facing scene camera, four eye-cameras, and infrared illuminators situated in the frame of the glasses [49], [50]. The recording unit is connected to the glasses and stores the gaze information on a removable SD-card.

Participants wore noise-canceling headphones to minimize the influence of noise on the recordings. They were seated roughly an arm's length from a monitor, wore calibrated eye-tracking glasses, and wore surface electrodes placed on their dominant forearm, see Figure 11. All the electrodes were linked to an open-source bioelectric signal acquisition device ADS_BP

[51], which was then connected to a computer. Seated a few meters behind the participant, the researcher noted down any significant occurrences during the trial by observing the live-view of the eye-tracker. If needed, participants were instructed between trials to reorient their heads when the eye-tracker failed to capture the full display of the monitor. The experiment consisted of ten five-minute-long trials, each having ten repetitions of each noise condition. Participants could take breaks between trials as they felt necessary.

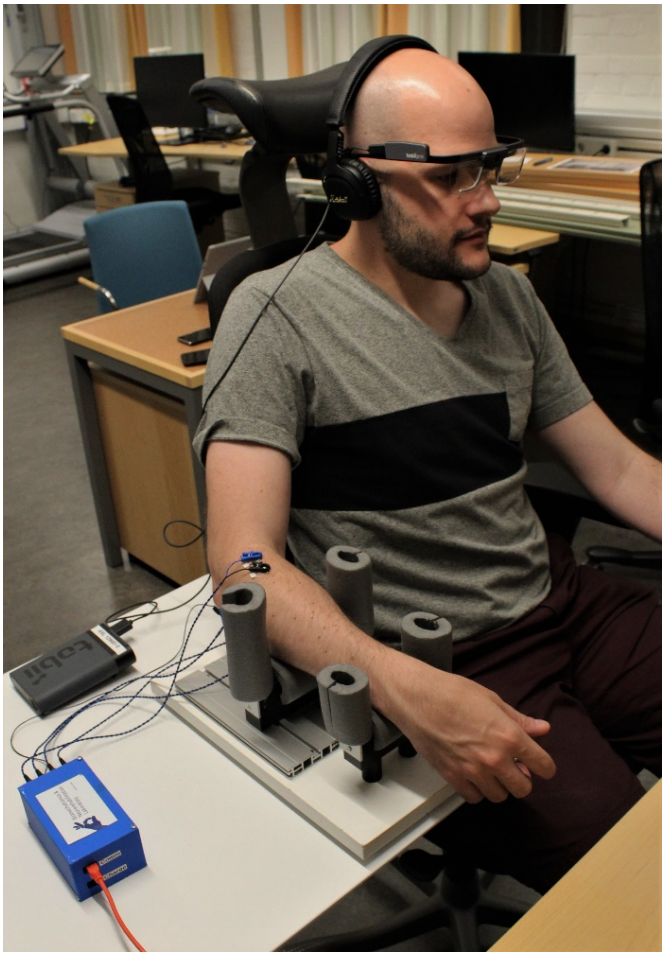

Figure 11. The experimental setup design. sEMG signals were recorded by four bipolar channels placed on the participant's forearm and transferred directly to the bioelectric signal acquisition device (an ADS_BP [51] enclosed in a blue-colored plastic casing). The wearable eye-tracker was mounted on the participant and was wired to the recording unit, which stored gaze-data and sent it wirelessly to a tablet used by the researcher seated a few meters behind the participant. Active noise-canceling headphones were placed on the participant to reduce any disturbances, and an armrest was used for the ease of movement and to elevate the arm from the table to reduce motion artifacts in the sEMG signal.

The virtual arm control interface

A modified version of the virtual reality environment (VRE), included in the research platform BioPatRec [39], was developed to portray the subject's volitional movements projected onto four virtual arms. The research platform was designed to develop algorithms for prosthesis control based on pattern recognition of myoelectric signals. It includes a virtual reality environment for real-time evaluation of various signal processing, feature extraction, and control algorithms. In brief, BioPatRec allows for decoding voluntary limb movements by extracting patterns from bioelectric signals obtained from EMG, by the strategical placement of recording electrodes near muscles responsible for moving the anatomical limb during intended movements.

Myoelectric signals recorded during participants' execution of opening and closing of the hand, along with wrist flexion and extension, were used for the real-time control of virtual reality (VR) arms in BioPatRec. A recording session consisted of three repetitions of a specific movement with three seconds contraction time, and three seconds relaxation period between contractions periods. The sEMG signal used for training the movement classifier was recorded with the sampling rate of 2000 Hz, the beginning and the end of the contraction time was trimmed by selecting 70% of the contraction time percentage in order to discard anticipatory relaxation and the delay between receiving instructions to move and executing the movement. Furthermore, the signal was segmented into 200 ms overlapping windows with a 50 ms time increment. Mean absolute value, zero crossing, slope sign changes, and waveform length were the features extracted from each movement's time window. The feature vectors, pertaining to each movement recording, were split into training (40%), testing (40%), and validation (20%) subsets. Combined with the resting state signals, the classification task consisted of five possible movement predictions and allowed for the movement of the virtual arm in the direction stated by these classes, with the displacement of two degrees per prediction. Discriminant analysis in a linear configuration with one-vs-one topology was used as an algorithm for pattern recognition, the same MPR settings as used by Ortiz-Catalan *et al.* [39].

The visual stimulus, included in BioPatRec, was developed using the OGRE3D open-source graphics rendering engine [52] and presented to the subjects on a 27-inch LCD monitor (W x H = 625mm x 453mm, 1920 x 1080 pixels, and 60 Hz refresh rate) at an arm's length distance. In each quadrant of the screen display were four 3D models (display resolution = 1920 x 1080 pixels) of gray-colored human-like arms on a black background, see Cover figure.

The degree of controllability over the virtual arms was varied by interfering with the movement classification of the control algorithm. This manipulation consisted of randomly

reclassifying MPR-predicted movement output in real-time, represented by a gray box seen in Figure 12. Thus, each movement prediction, based on sEMG input-signal, faced a certain reclassification probability (or noise level) of being changed into a randomly selected movement classification, distinct from the MPR-prediction, from the set of utilized movements in the prediction strategy. Based on the ongoing noise condition, see Table 1, the noise level of a VR arm was set to 0%, 25%, 50%, or 75%. The assigned noise level X and a uniformly distributed randomly generated number *rnd* in the interval [0, 1] determined whether or not a random reclassification of a prediction occurred, i.e., $X > rnd \sim U([0,1])$. As an example, a 50% noise level assigned to a VR arm represented a 50% probability of changing a closed hand prediction to another randomly selected movement, i.e., either open hand, wrist extension, wrist flexion, or resting state. Additionally, VR arm control is further affected by the algorithm's inherent classification accuracy, which could result in an erroneous prediction or misclassification of the user's intended movement.

At every ~50 ms, three movement commands were generated in this manner, along with a single unaltered copy of the MPR-based prediction, and finally saved to a movement command storage to be executed by the VR arms. Meaning that at least one VR arm consistently executed the predicted movement of the classifier while the other three could have an altered prediction, see Figure 12. Regardless of the assigned noise level, the resting-state command was executed on all the VR arm whenever there was a resting state prediction. This exception was implemented to avoid constant reclassifications when the user performed no movements. The overall idea behind the noise implementation was to mimic how the MPR-based algorithm misclassifies an sEMG input signal and influence the classification accuracy of the controller.

Table 1. Three different noise conditions randomly assigned to every ten seconds of a five-minute-long trial. At the onset of every condition, random permutation determined how noise levels were mapped onto each VR arm throughout the next ten seconds. Unaltered MPR-based movement prediction is represented by 0%, while > 0% signifies the probability of changing an MPR-prediction to another class in the set of utilized movements.

	Noise level mapping to a random ordering of the VR arms			
Noise condition				
Low	0%	25%	25%	25%
Medium	0%	50%	50%	50%
High	0%	75%	75%	75%

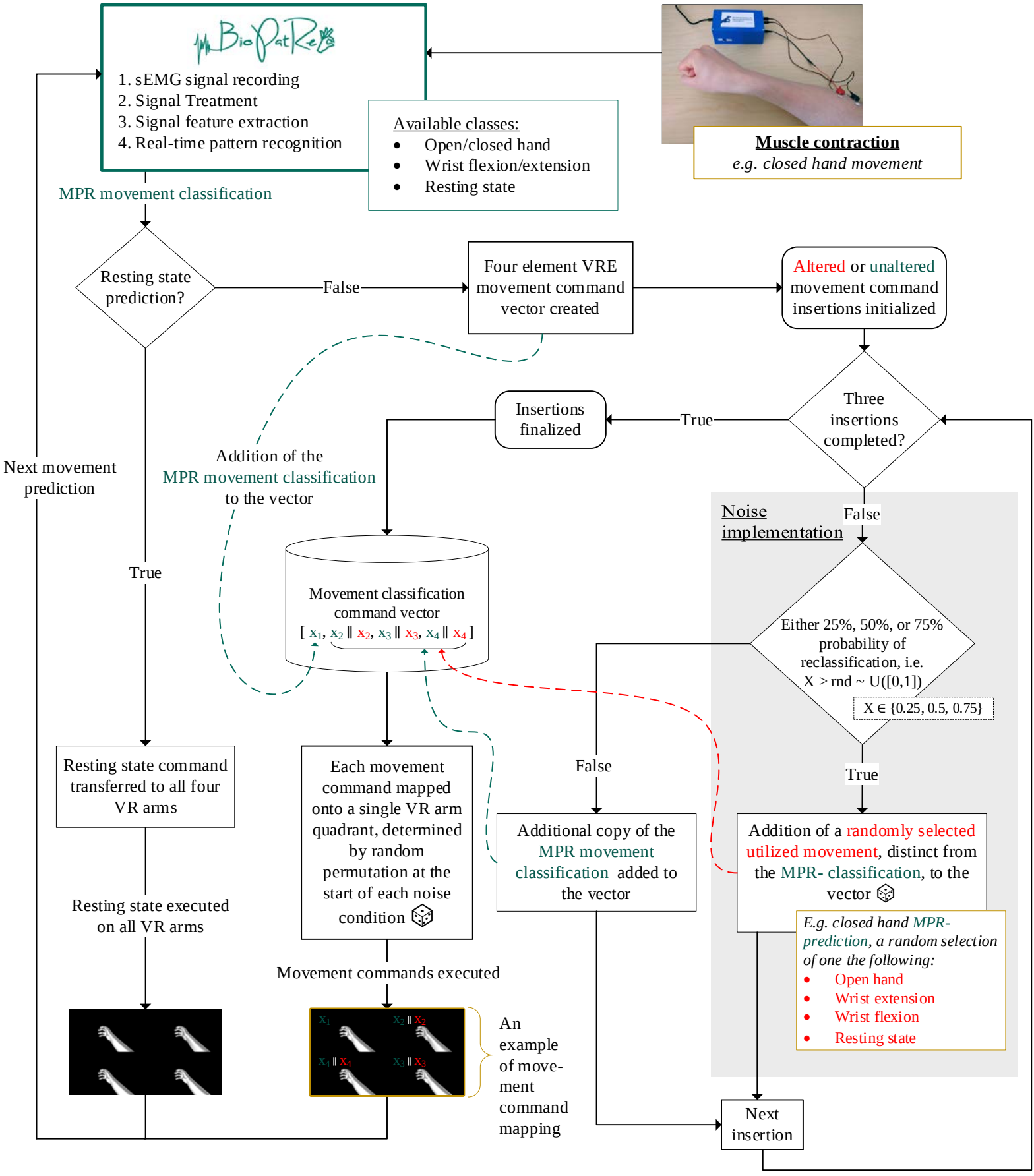

Figure 12. Flowchart representing the dynamics of the virtual arm control interface. The gray box on the right shows how the implemented noise levels (or random reclassifications) affected each movement prediction made by the MPR-based VR arm controller, making the participants control over the VR arms variable. Whenever the classifier made a resting state prediction, no movement was executed by any of the arms. However, whenever a movement prediction was made, a movement command storage was generated, followed by the execution of the stored commands by the VR arms on-screen. At least one copy of the movement classification made by the MPR (noted in **green**) was stored in the command vector along with movement reclassifications due to the assigned noise level (noted in **red**). The likelihood of an altered prediction being added to the command vector was dependent on a specific noise level randomly mapped to each VR arm quadrant during the ongoing noise condition of each trial, see Figure 13 and Table 1.

Design

The experiment was developed as an extension to the modular platform BioPatRec and therefore written in the programming language MATLAB, with support of the Psychophysics toolbox [53]. At the start of each five-minute-long trial, a white fixation cross on a black background appeared on the center of the monitor. When ready, each participant pressed a key with their non-dominant hand on a keyboard to initiate the experimental trial. After the keypress, a visual stimulus consisting of four identical virtual arms on a black background positioned symmetrically on each quadrant of a monitor was shown, see Figure 13. The participant's task was to make one of the four virtual arms flash red for 200 ms (as seen on the Cover figure) as often as possible throughout each trial by maintaining continuous movement of the VR arms. Detection of each red color flash on a VR arm was then indicated, by the participant, with the press of the spacebar-button on a keyboard, using the non-dominant hand. The task was repeated until the white fixation cross appeared on the screen again, indicating that the next trial could be started.

A sequence of 60 separate time points was generated before the start of each trial, where a VR arm flashing red was set off at each point. Only a pair of red flashes on VR arms could occur within each ten-second noise condition period of the trial and with a minimum of three-second interval separation between them. Each pair of red flashes on VR arms had a 50% chance of either occurring on the first, fourth, or seventh second of each ten seconds in a trial (randomly selected), or on the second, fifth, or eighth second of the period. A red flash on a VR arm would not occur on a predetermined time point unless a VR arm was moving at that time. The number of red flashes on a VR arm was balanced over all four possible noise levels. In other words, fifteen flashes occurred on a random VR arm with the assigned noise level of 0%, 25%, 50%, and 75% noise level, therefore 60 flashes per trial.

Three noise conditions were used in the trials as seen in Table 1 and Figure 13, where the control of three virtual arms (selected by random permutation) had either 25%, 50%, or 75% chance of being decreased by reclassifications to the output prediction of the MPR-algorithm during each ten seconds of the trial. This impaired control consisted of reclassification of the MPR-based movement prediction to another classified movement, which was distinct from the prediction. Therefore, the control interfaces' likelihood of misclassifying the participant's movements was varied and subsequently made the participant's voluntary movement either less or more congruent with the real-time movement of the three VR arms. However, a single VR arm in all of the noise conditions consistently executed the unaltered MPR-based movement

prediction; therefore, its movement commands had a 0% chance of being reclassified. Before the start of each trial, a sequence of 30 randomly permuted noise conditions (10 occurrences of each condition) was generated and then used in the upcoming trial. Moreover, at the start of each ten-second noise condition within a trial, noise levels were randomly mapped onto each VR arm. A single VR arm was assigned no reclassification probability, with the remaining VR arms being assigned a noise level matching the ongoing noise condition of the predetermined sequence, see Figure 13.

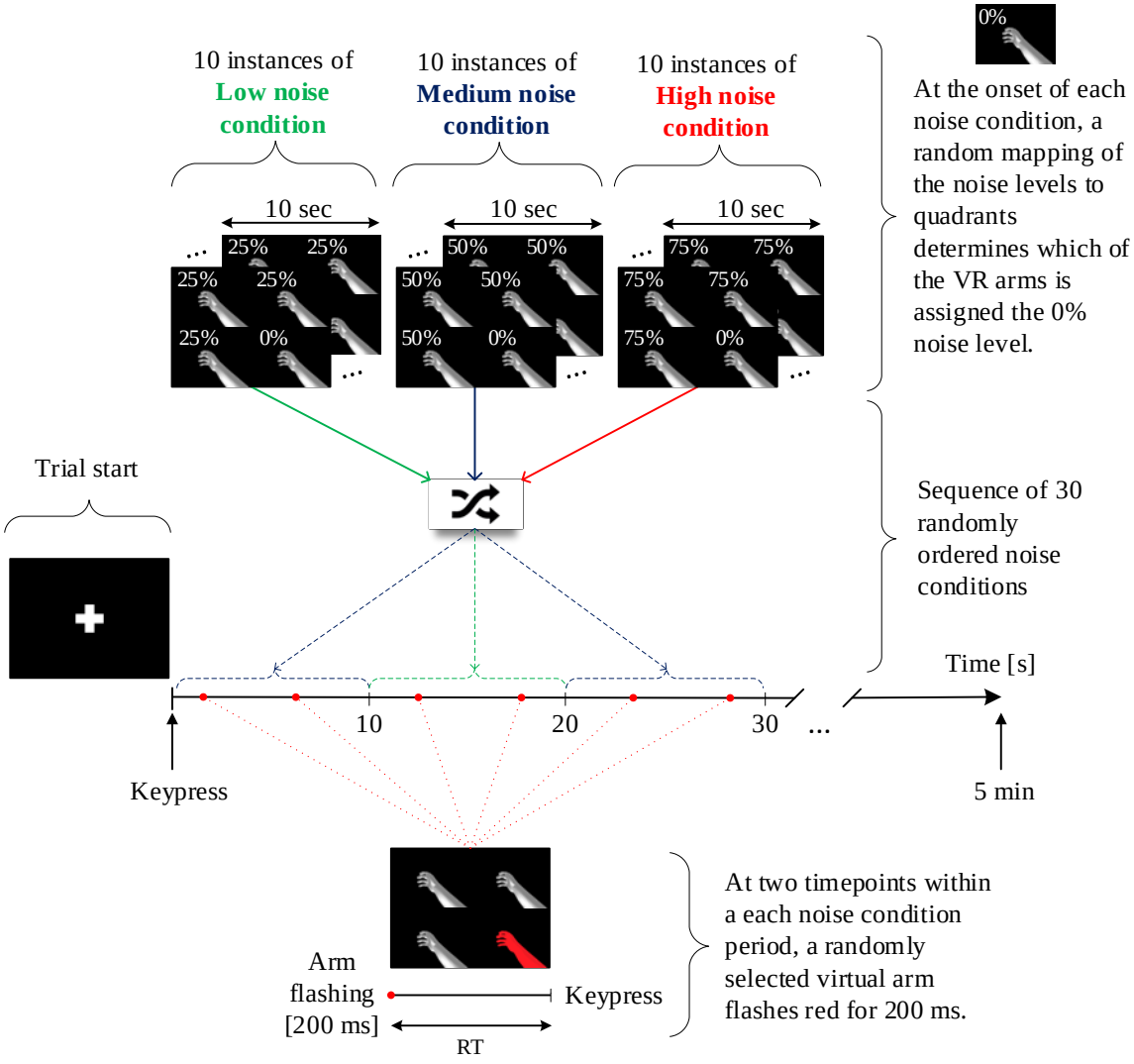

Figure 13. Graphical representation of a single trial timeline design. The trial starts with the appearance of a white fixation cross, followed by the appearance of the four virtual arms in each quadrant of the screen after a keypress. Each ten-second period of a trial was assigned a random noise condition, as seen in Table 1, where the three possible noise conditions for the virtual arms (low, medium, and high), along with the onset of the VR arm flashing red is depicted. Noise level values were not visible to the participant on the monitor, as seen in this figure.

Importantly, however, the instructions communicated to the participant were intentionally made to differ from the narrative of the actual experimental design as described in this section. The discrepancy consisted of withholding information about the noise implementation of the VR arm controller, and how the red flashes on the VR arms were set off. Further explanation of the instructions given to the participants is described in the following section.

Procedure

Each participant was tested during a single visit to the BNL laboratory. Before arriving at the lab, the participants were advised not to wear mascara which could obstruct the eye-trackers view of the eye, wear a short-sleeved shirt to facilitate the placement of the surface electrodes, wear corrective optics if needed, and to use hairpins to keep long hair or bangs out of the trackers view. When arriving at the lab, the participants signed the relevant consent forms, which delineated their task and the procedure of the experiment. A brief questionnaire about their handedness [48], and whether they had been diagnosed with eye-alignment abnormalities or underwent eye-surgeries was filled out. Information about the measuring equipment was provided to the participants: during the trial, they would be able to control a virtual limb via muscle activity recorded from the sEMG electrodes and that their eye-movements would be recorded throughout the trials.

The equipment set-up leading up to the trials started by seating the participant in an office chair with a height-adjustable headrest in roughly an arm's length in front of a computer monitor, with the dominant arm resting comfortably on an armrest, and the other arm within reach of a keyboard. Four channels, each consisting of two monopolar Ag/Ag-Cl adhesive surface electrodes and separated by approximately 2 cm, were equally spaced around the proximal third of the dominant forearm. The first channel was placed along the extensor carpi ulnaris muscle, which was located by palpation after instructing each participant to extend their wrist to reveal the position of the muscle underneath the skin. Finally, a single reference monopolar electrode was placed on the apex of the elbow of the dominant arm. This electrode placement, used by Ortiz and others in 2013 [39], was shown to provide ~ 60% real-time classification accuracy of various hand and wrist movements based on two real-time tests provided in BioPatRec. After that, sEMG signals were recorded for the training of the pattern recognition classifier, using roughly 70% of their voluntary muscle contraction, with three second relaxation period between three-second contraction time repetitions of each movement.

To visually assess whether the controller could correctly predict each classified movement and to allow the participant to get familiarized with the control, a short practice session with a single VR arm displayed was conducted. The practice trial was repeated until the execution of all the trained movements with the VR arm was possible. If the controller was unable to classify a movement, a new classifier training recording session was repeated as an attempt to get the controller to generate more accurate movement prediction.

An appropriately sized nose pad was chosen to align the participants' eye to the middle of the glasses frame and to ensure the best fit. To ensure that accurate eye-tracking was obtained, a calibration procedure was followed where the participant looked the middle of a black and white bullseye on a plastic card at a roughly meter distance. Next, the tracking quality was validated in real-time by observing the live-view of the camera-feed on a wirelessly connected tablet to the eye-tracker. Participants were instructed to look at four white markers on each corner of the monitor, one at a time in a clockwise manner. Tracking was deemed satisfactory if the real-time gaze-point corresponded to the location of the white marker at which the participant simultaneously looked at when instructed. When needed, participants were instructed to adjust their head pitch for the full monitor display to fall within the view of the scene-camera. Correct head posture resulted in capturing most gaze-data relating to the observation of the displayed VR arms.

After finalizing all the necessary preparations, the participants were given their task instructions. No information about the varying degrees of control over the virtual arms, due to the mapped noise levels, was conveyed to the participants. They were kept ignorant of this fact to not bias their attention towards their VR arm controllability, but rather examine the potential automatic attentional allocation towards it during a simple detection task. The only task-related information given included instructions to trigger as many red flashes on a single VR arm throughout the trial. In order to do so, all available VR arm movements had to be utilized to move them into a randomly generated and unknown posture to set off a red flash on a VR arm. Additionally, no red flash of a VR arm would occur if the arms were not kept under continuous movement, and the red flash would always occur on a randomly selected VR arm amongst the four. As soon as they would see the red flash on a VR arm, they were instructed to respond with a press of a key on a keyboard.

Contrary to the instructions given, the randomly generated posture used to trigger the brief color change of a VR arm was not implemented in the experimental design. These instructions were used as a cover story to motivate participants to maintain motion on the VR arms during a trial and to give their task a less monotonous purpose rather than only requesting

free movement of the arms. Finally, they were misled to believe that the purpose of the experiment was to study response time to the red flash of a VR arm while the eye-tracking data was recorded as supplementary data to examine visual attention during the execution of that detection task. The real objective and design of the experiment were clarified to each participant during a post-experiment debriefing session.

Data analysis

For gaze data analysis, the software tool Tobii Pro Lab (Tobii AB, Danderyd, Stockholm, Sweden) was used to extract data relating to eye-fixations located on four areas of interest (AOI, W x H = 840 x 561 pixels), each surrounding a VR arm in each screen quadrant, as seen in bottom of Figure 14. The rectangular-shaped AOI was placed around each virtual limb to aggregate statistical data relating to eye-fixations that were positioned on a virtual limb. A video, captured by the eye-trackers front-facing scene-camera, included a mapped gaze point on each 20 ms frame-capture of the recording. Since the visual stimulus of interest was presented on a stationary surface of a monitor and not on a dynamically changing scene, it was decided to map all gaze data from the video recording onto a coordinate system of a static reference image (display resolution = 4577 x 3079 pixels). The scene at which the participants looked in each trial, a desk with a monitor displaying four virtual limbs in each quadrant, were the contents of the reference image, as seen on the right in Figure 14.

With the use of the software's automatic gaze mapping feature, each gaze point from a single video frame was mapped onto a reference image of the scene with a specific confidence value. White markers were placed on every corner of the monitor to include prominent features in the reference image for the facilitation of detection by the image detection algorithm used in the automated gaze mapping feature [54]. Additionally, to further enhance the accuracy and precision of the resulting automatic gaze mapping data, a fixation-by-fixation search through each participant fixation-filtered gaze recording was done to manually re-map any erroneously mapped gaze-points made by the algorithm, as seen to the right on Figure 14.

Classification of eye-fixations was done with a velocity threshold identification (I-VT) filter included in the eye-tracker analysis software [55], [56, pp. 87–90]. If the recorded angular velocity value of a single gaze sample was below 30°/sec, it was classified as a fixation; otherwise, it was classified as a saccade. Subsequently, consecutive gaze samples classified either as fixations or saccades are collapsed into larger segments by the merge function. Merging of adjacent fixations was based on two-parameter criteria: temporal separation of less than 75 ms and angular of less than 0.5°. Furthermore, eye-fixations with a duration of less than

60 ms were reclassified as non-fixation gaze samples. These data constraints are applied to merged samples to filter out blinks and microsaccades, also to mitigate the fragmentation of more prolonged fixation by interference [57]. A flowchart in Figure 15 shows the gaze data processing pipeline by the I-VT filter and the merge function.

Figure 14. Snapshot from the user interface in Tobii Pro Lab software showing a red circle denoting the recorded gaze point on a single frame in the scene-camera recording of the wearable eye-tracker (left), and the reference image on which gaze points from the recording were mapped onto (right). Furthermore, the gray circle shows the software's attempt at automatically mapping the gaze point, and the red circle with the letter M in its border was the manual remapping of the gaze point with a point and click of a mouse. Four equal-sized rectangular areas of interest (bottom) were placed symmetrically around each VR arm in a quadrant to classify whether an eye-fixation was located on a virtual limb or not.

Eye-fixation duration and count within four different AOI surrounding each virtual arm in their respective quadrant on the screen were used as outcome measures. Besides eye-fixations, response time to visual detection of the red color flash on a VR arm was recorded and delimited by the moment when the virtual arm had reverted its color from red to gray and until a keypress was registered, as portrayed in the bottom of Figure 13. All data analysis on preprocessed gaze-data and response time was performed using the software MATLAB and the software environment R. All references to participant-specific data were done by using non-identifiable codes, starting from AB03 to AB08. In order to test for a statistically significant

difference between noise level groups (0%, 25%, 50%, and 75%) of the gaze data and reaction time, the non-parametric Kruskal-Wallis test was implemented. A significance level of $\alpha = 0.05$ was used, and a Bonferroni correction to compensate for multiple pairwise comparisons using Dunn's test with data from the same sample.

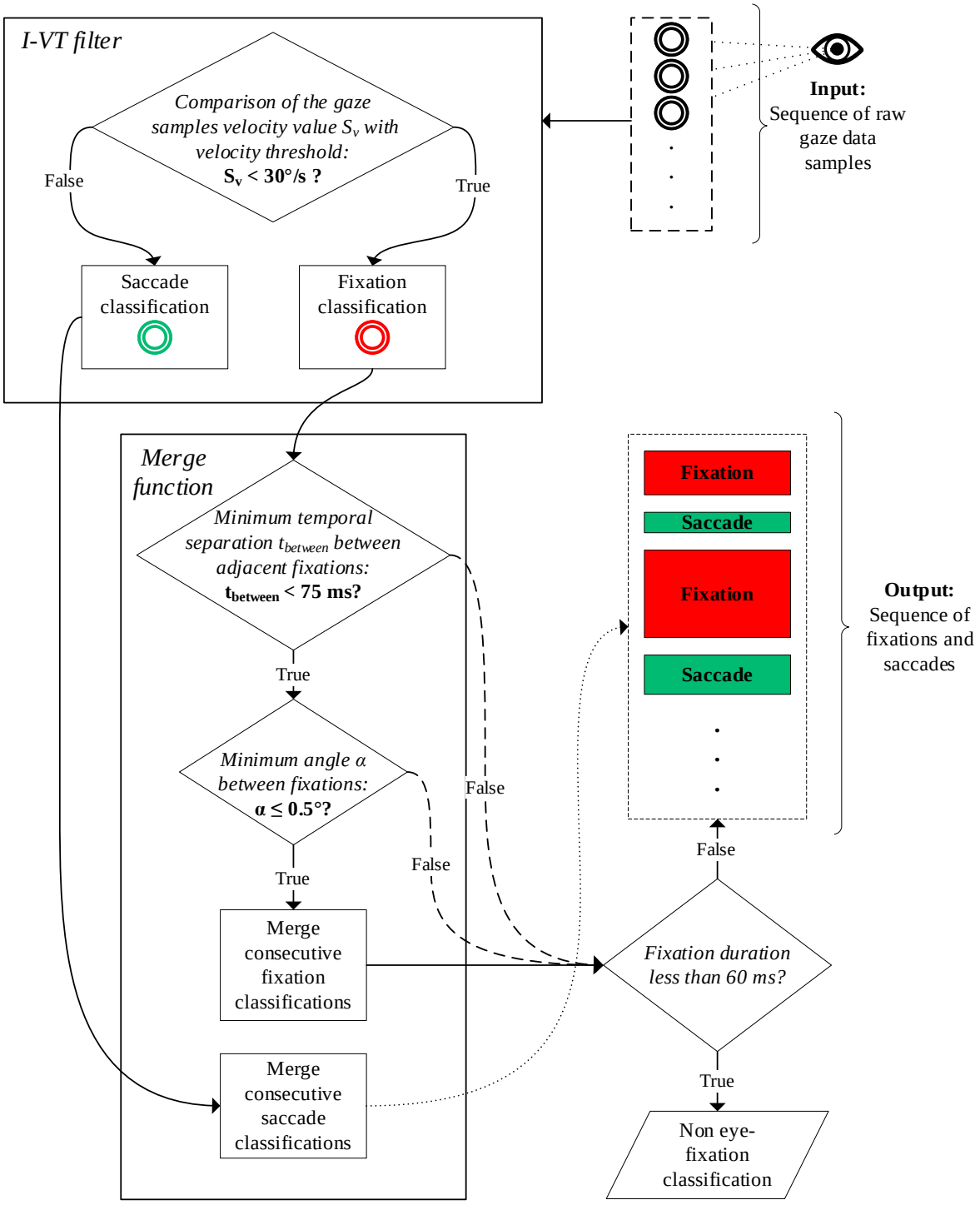

Figure 15. A flowchart illustrating how the gaze data samples were classified due to the velocity threshold filter (I-VT) and merge function.

4 Results

The following discussion is about gaze-tracking data and reaction time analysis. All data is represented graphically by either bar plots, box plots, or raincloud plots. A raincloud plot [58] is a data visualization method that combines the data distribution information from a boxplot, jittered data points, and a 'split-half' violin plot. In the middle of each raincloud plot, a boxplot is drawn with the mid-line of each box representing the median of the distribution, the lower border of the box the 25^{th} percentile, and the upper one the 75^{th} percentile. From the bottom and top edges of the box, a whisker reaches the most extreme data point that is not classified as an outlier (represented by red circles). One half of a violin plot is overlaid on top of the boxplot, which illustrates the concentration of the distribution with respect to the values of the dependent variable, its width representing the frequency of samples. Next to the density function, raw data points are jittered along the y-axis to prevent overlapping and, therefore, further illustrating the density of the distribution. Finally, each column in the following bar plots represents either the number of eye-fixations or their total duration within a specified condition.

A single asterisk symbol '*' was used to represent a significant difference in a raincloud plot based on a probability value of $p \leq 0.05$, while two, three, and four asterisk symbols signify a statistically significant difference based on values $p \leq 0.01$, $p \leq 0.001$, and $p \leq 0.0001$, respectively.

4.1 Eye-tracking data

Each participant demonstrated a unique gaze-behavior strategy as indicated by their eye-fixation distribution across all the trials on the computer monitor and made apparent when comparing each participant's gaze-fixation distribution.

4.1.1 Visualization of gaze data

To graphically represent the distribution of attention over the visual stimuli (i.e., the four virtual arms), six heatmaps were prepared [44, pp. 275–287], [59] of the absolute fixation duration for all ten trials conducted by the participants as seen on Figure 16. A heat map adds up, one-by-one, eye-fixation durations that share the same pixel coordinates on the reference image and assigns a color temperature proportional to the duration of each fixation, warmest color or red

representing the maximum value. Furthermore, all duration points in the vicinity of a fixation point are added together to create a smooth color gradient instead of scattered colored dots.

As the heatmaps in Figure 16 indicate, each participant appears to have adopted a distinct visual behavioral pattern during each trial. Meaning that some tended to have more centralized attention towards the visual stimuli (AB03 & AB06), spending more time looking at the center of the screen while using their peripheral vision to detect the red blinks of the VR arms, whereas others actively moved their eyes around the display of the screen (AB04, AB05, AB07 & AB08), which was evident by a denser fixation distribution over each VR arm screen-quadrant.

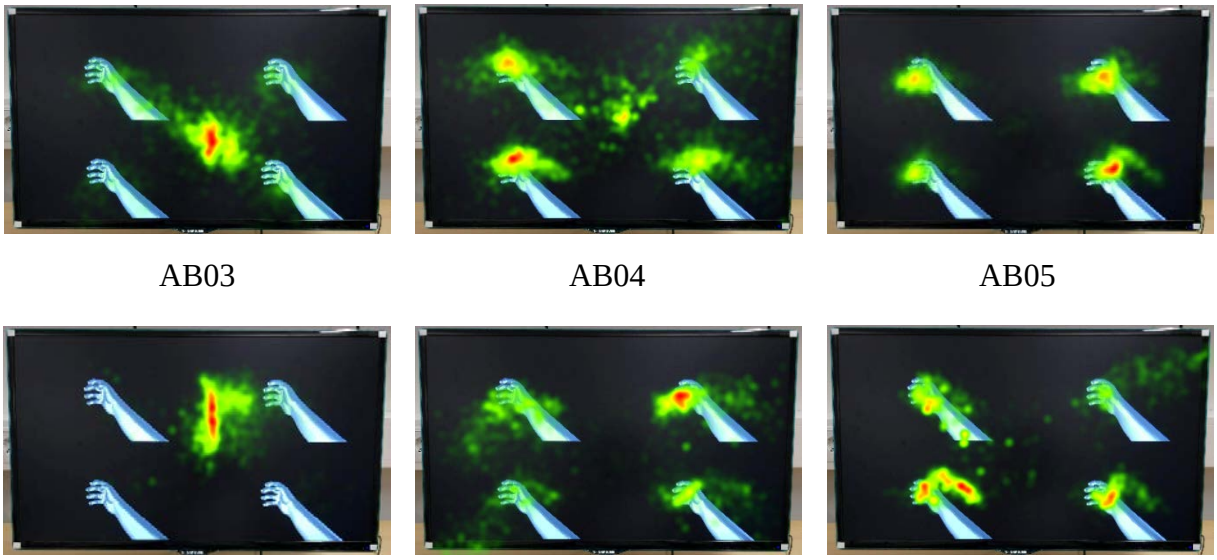

Figure 16. Each participant fixation duration heatmap across all trials. A single heatmap portrays the accumulated time spent by a participant fixating at different areas of the visual stimulus. Fixations, one-by-one, are assigned a value that is proportional to their durations, mapped to the reference image, and then summed together with other fixations having similar coordinates. All adjacent fixation durations are added together to form a color gradient, where red, or the warmest color, is assigned to the highest summed absolute value of fixation duration.

4.1.2 Fixation duration devoted to AOI

The total fixation duration made by all participants on each AOI on the screen, shown in Figure 17, served as further quantitative analysis and support for the data visualized on the heatmaps in Figure 16. The center-focus fixation pattern exhibited by participant AB03 and AB06, and seen on the heatmaps in Figure 16, corresponds with the fixation duration data in Figure 17. The former participant spent relatively similar time fixating on each AOI, while the latter spent

most time fixating on the first quadrant AOI and with considerably less time spent looking at the other three AOI. For the rest of the participants, the fixation durations were divided more evenly across each AOI, with no participant spending less than 200s fixating on each AOI. Additionally, only the distributions of fixation durations (made by all participants) associated with Q1 and Q4 were not significantly different (see Appendix I for further discussion).

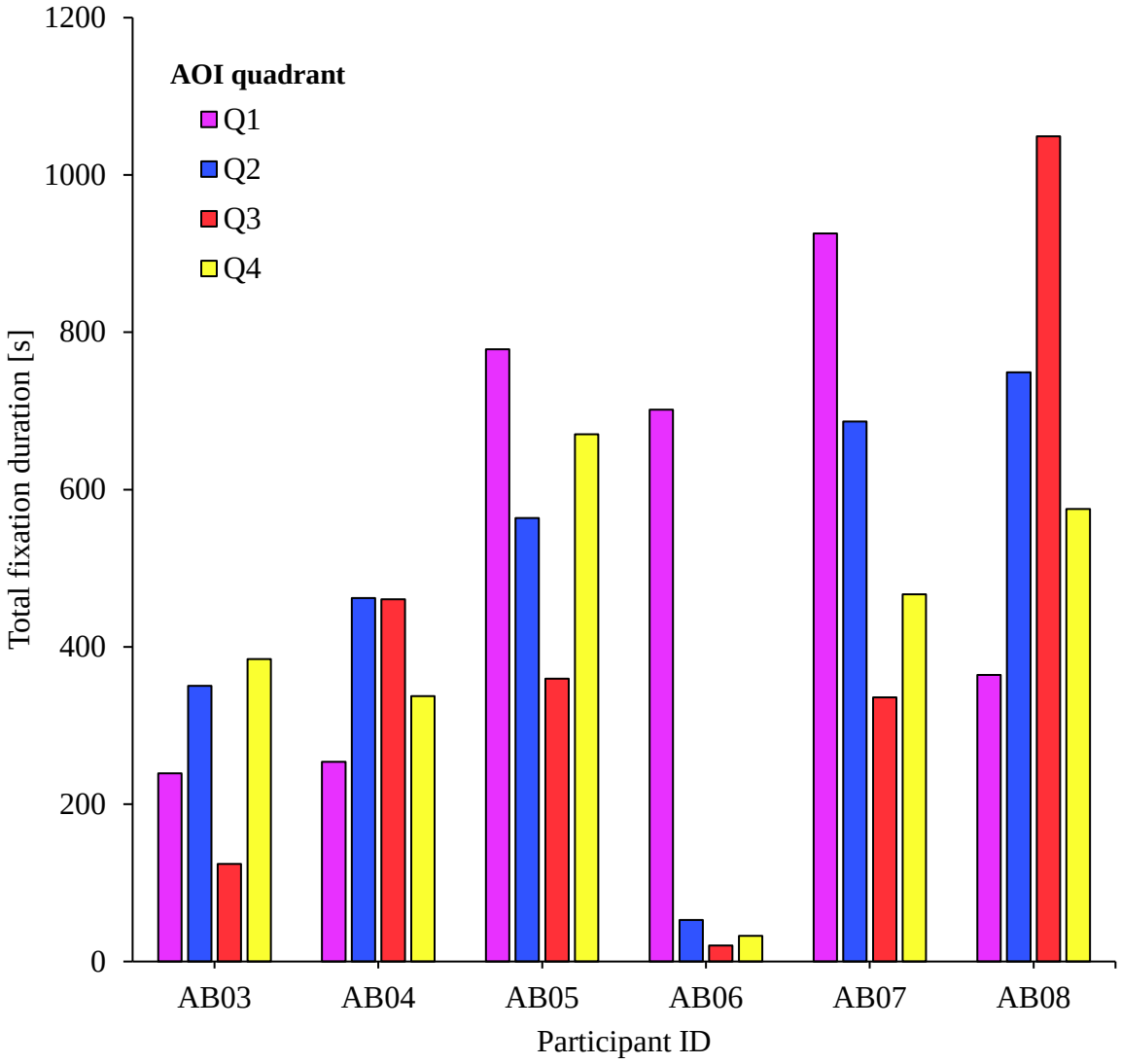

Figure 17. Total fixation durations made by each participant, across all trials, on the four AOI situated on each quadrant of the visual stimulus. The **first** AOI, defined as 'Q1' on the graph, is positioned in the upper right corner, followed by the **second**, **third**, and **fourth** AOI quadrants, positioned in a counterclockwise manner around the middle of the computer screen, as in the 2D Cartesian coordinate system convention. Each bar color represents the color-coding of AOI, as seen in Figure 14.

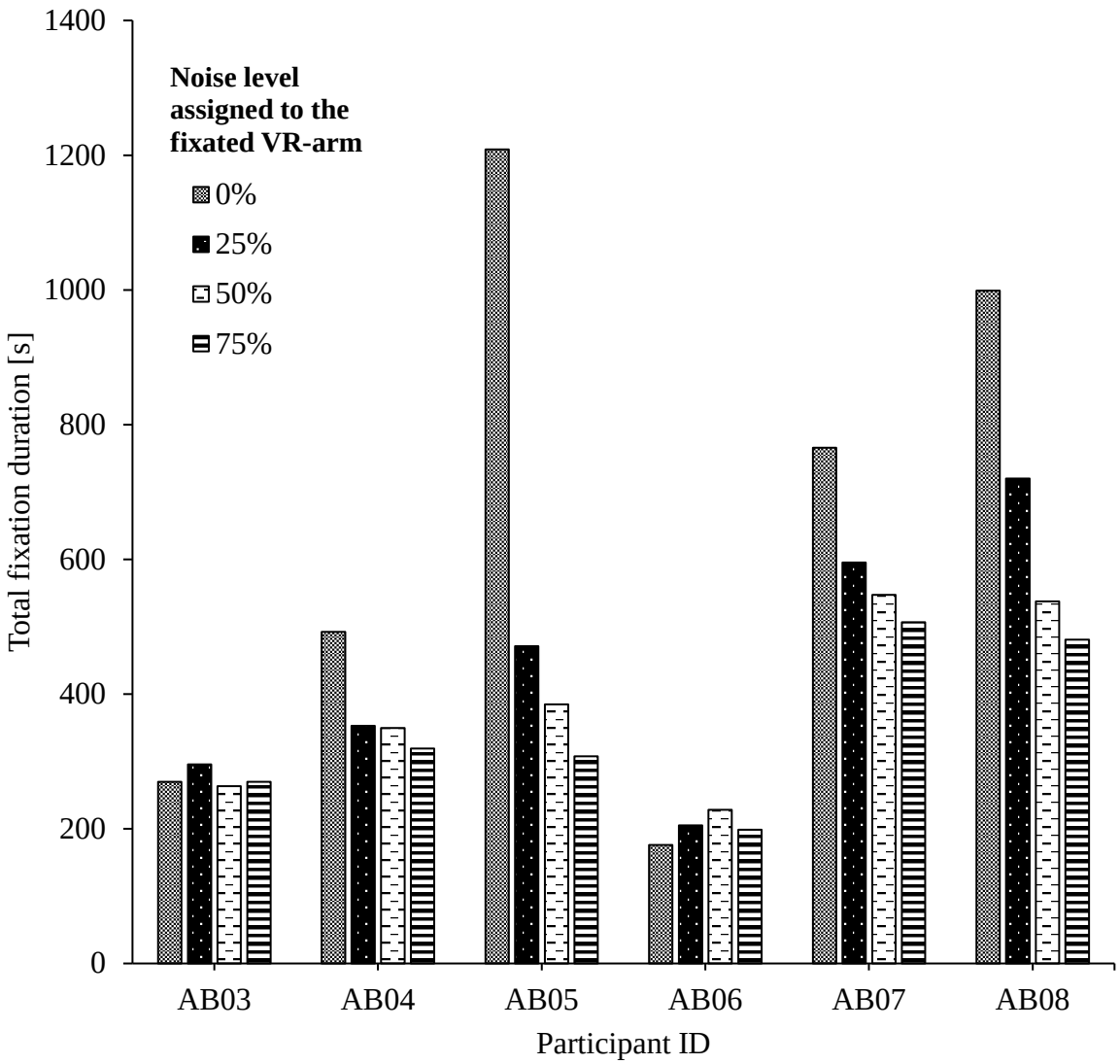

Figure 18. Total fixation duration grouped by each participant, across all trials, with each bar representing the assigned noise level to the VR arm occupying an AOI at the time of fixation.

Participant's degree of controllability over a VR arm, determined by each noise condition occurring throughout each trial, seemed to influence the time spent looking on an AOI surrounding a VR-am. In the case of participants who did not exhibit a center-screen oriented eye-fixation pattern, the increased controllability over a VR arm (or low level of noise added to the VR arm controller) appeared to affect the amount of time fixated on AOI. For every participant except AB03 and AB06, longer total fixation duration was devoted towards an AOI containing a VR arm with unaltered MPR-movement commands, or 0% noise level, compared to other AOI surrounding an VR arm with increased reclassification probability (either 25%, 50%, or 75% probability of movement reclassification), as seen on Figure 18. However, in the case of AB03 and AB06, a comparable amount of total fixation duration was spent on VR arms at each noise level. It might be that the red flash onset on a VR arm, balanced

across all possible noise levels, automatically attracted their attention instead of the concurrent controllability level on each VR arm, as indicated by the fixation duration data. In the light of the results mentioned above (i.e., see Figure 16 & Figure 18), the gaze pattern of participants AB03 and AB06 was deemed uniform and divergent compared to the other participants. The overall fixation position recorded from these participants might suggest that the visual stimulus did not have a meaningful impact on their gaze behavior; thus, a decision was made to exclude their recorded gaze data and reaction times from additional inferential statistical analysis.

4.1.3 Fixation count and duration within noise conditions

To further compare the effects of added noise level to a VR arm against an unaltered MPR-controlled VR arm, the eye-fixation data within all the noise conditions were analyzed.

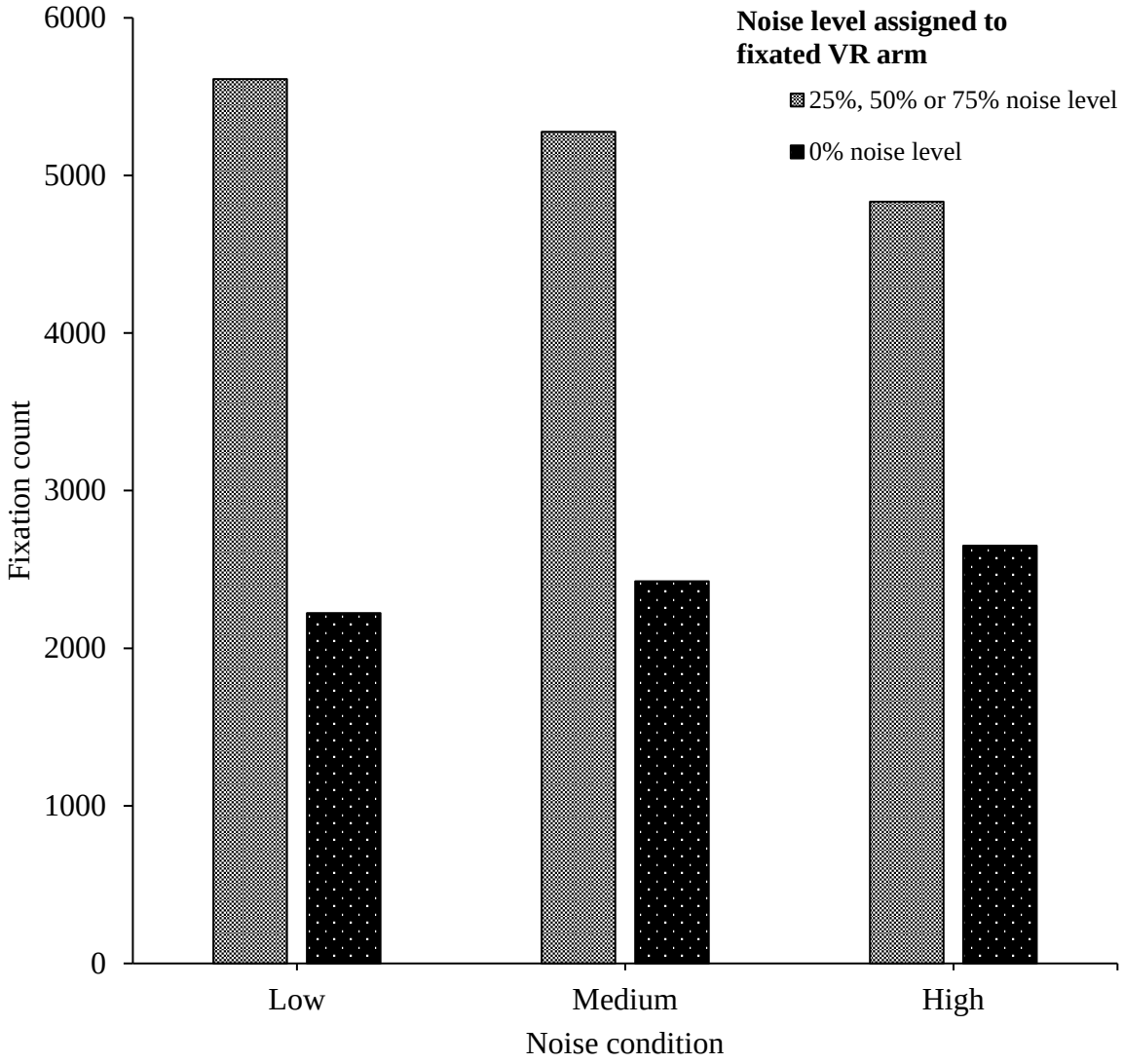

Figure 19. The number of eye-fixations grouped by the ongoing noise condition and by whether the fixated-on VR arm was assigned noise (25% probability for low noise, 50% for medium noise, and 75% for high noise) or not (0% probability).

The results indicate that during each noise condition, the participants fixated for a longer time on quadrants that had noise assigned to them, compared to the time spent on a single random quadrant containing a VR arm without noise. The difference in fixation duration and count might be due to the three times larger area occupied by the three noise-assigned VR arm compared to the single VR arm without noise assigned. Resulting in a high likelihood of a participant looking at a noise assigned VR arms due to the majority of the area they occupy on the visual stimulus. The total fixation duration and the number of fixations for all participants, dependent on whether there was noise implemented or not on the VR arm controller, can be seen on the following bar plots in Figure 19 and Figure 20.

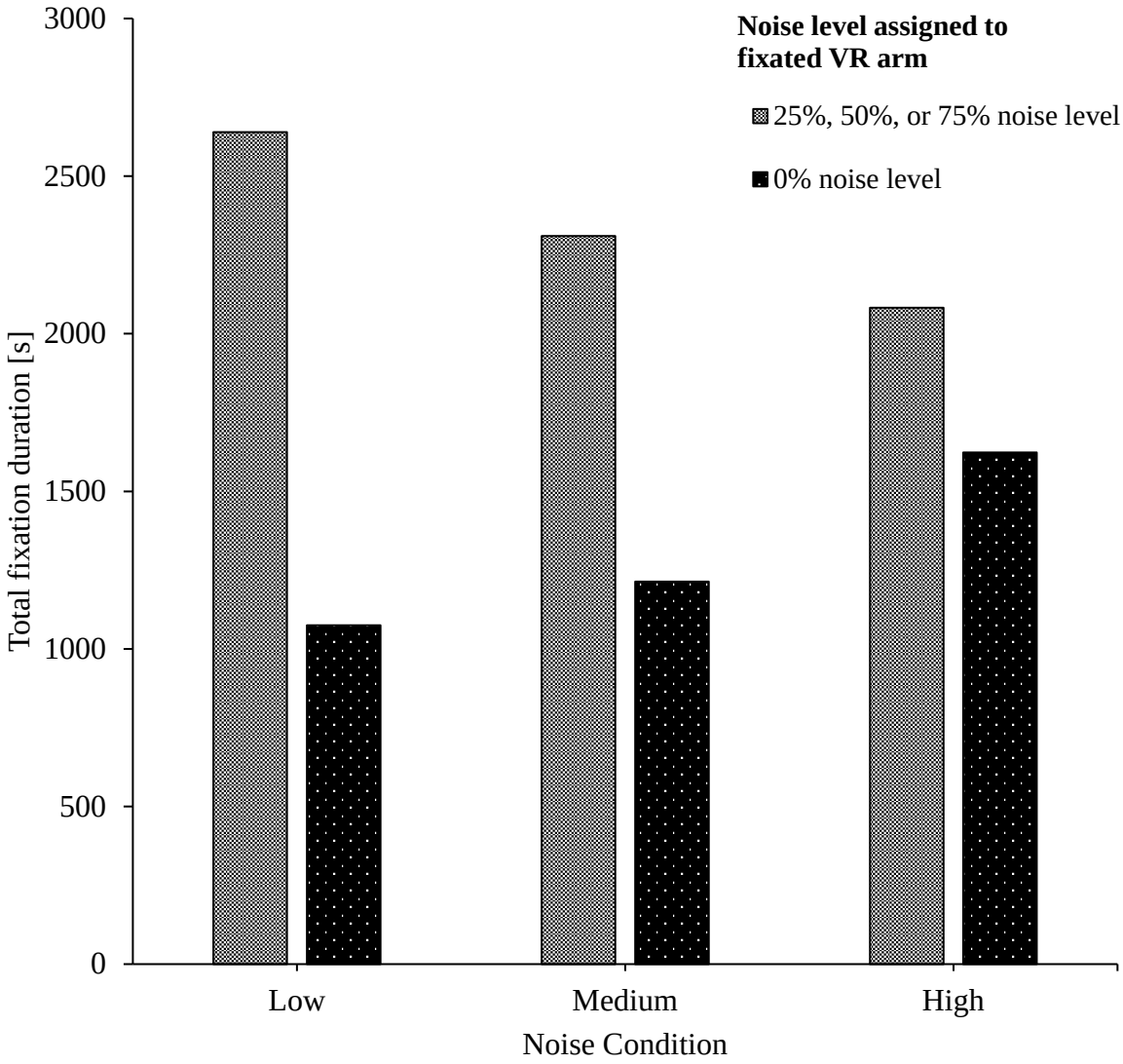

Figure 20. The total duration of eye-fixation grouped by the ongoing noise condition and by whether the fixated-on VR arm was assigned noise (25% probability for low noise, 50% for medium noise, and 75% for high noise) or not (0% probability).

4.1.4 Fixation duration distribution comparison between assigned noise levels

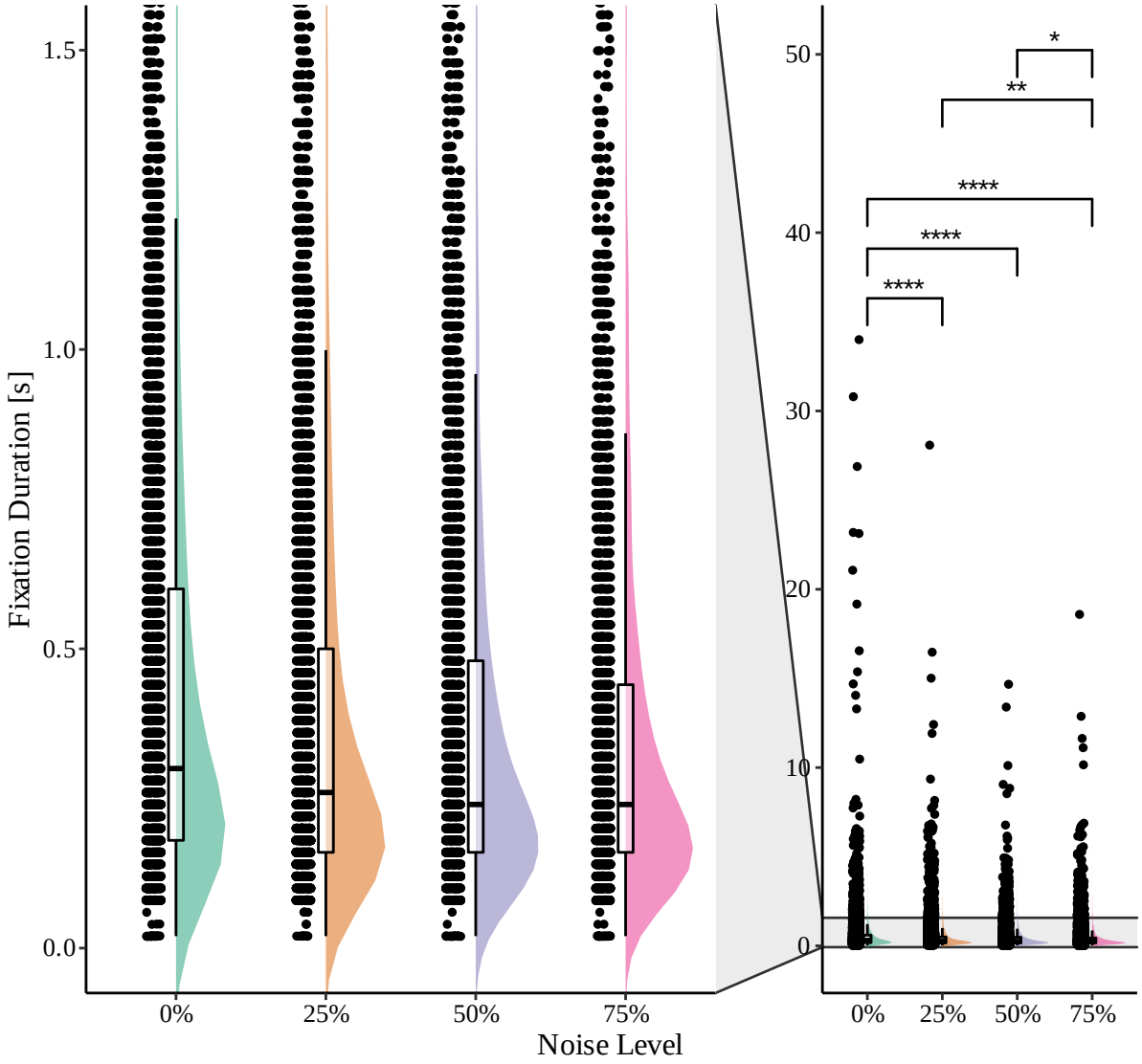

Figure 21. A raincloud plot of the eye-fixations distributions grouped by each noise level assigned to the fixated VR arm at the time of the eye-fixation. The overall gaze data distribution with outlier values and results of pairwise comparisons can be seen (right), along with a zoomed-in view of the densest part of all of the four distributions (left). Asterisk symbol signifies a statistical difference between two different levels of the independent variable, or assigned noise level, while the absence of asterisk symbols signified the lack of significant difference.

Finally, it was decided to compare the fixation duration distribution of all possible assigned noise level values. To verify whether each fixation sample originated from the same distribution, a nonparametric test for significance, Kruskal-Wallis, was conducted on all four noise level groups (0%, 25%, 50% & 75%). The results from the test showed that there was a statistically significant difference in fixation durations between different noise groups (rejection

of the null hypothesis that all samples come from the same distribution), **$\chi^2(3) = 152.59$, $p < 0.001$, & $n = 17914$**. Pairwise comparisons, using Dunn's test, of each noise group showed that there was significant difference between the fixation duration distribution of the 0% noise level group and the other three noise levels, i.e. 25%, 50%, and 75% (all having $p \leq 0.0001$, adjusted using the Bonferroni correction), as well between 25% and 75% ($p \leq 0.01$), and with $p \leq 0.05$ for the comparison between 50% and 75%, see Figure 21. The results suggest that the samples from these above groups do not come from the same distributions, which seems to suggest that the participants automatically looked for a more extended time on VR arms that they had more control over. However, no significant difference was detected between the fixation distributions of the 25% and 50% noise level groups ($p = 1$).

4.2 Reaction time data

Lastly, the reaction times recorded from each participant's detection task were analyzed, that is when they responded to the red flash on a VR arm during the experimental task with a push of a keyboard button. Each reaction time was recorded as the time interval between the disappearance of the red flash and the subsequent press of a button by a participant, as can be seen in Figure 13. The following boxplot in Figure 22 shows the reaction time distribution for each participant, grouped by the concurrent noise level. Out of maximally 3600 possible red flashes on VR arms, 221 were either not responded to within 2.5 seconds after the appearance of the red flash or did not appear due to motionless VR arms.

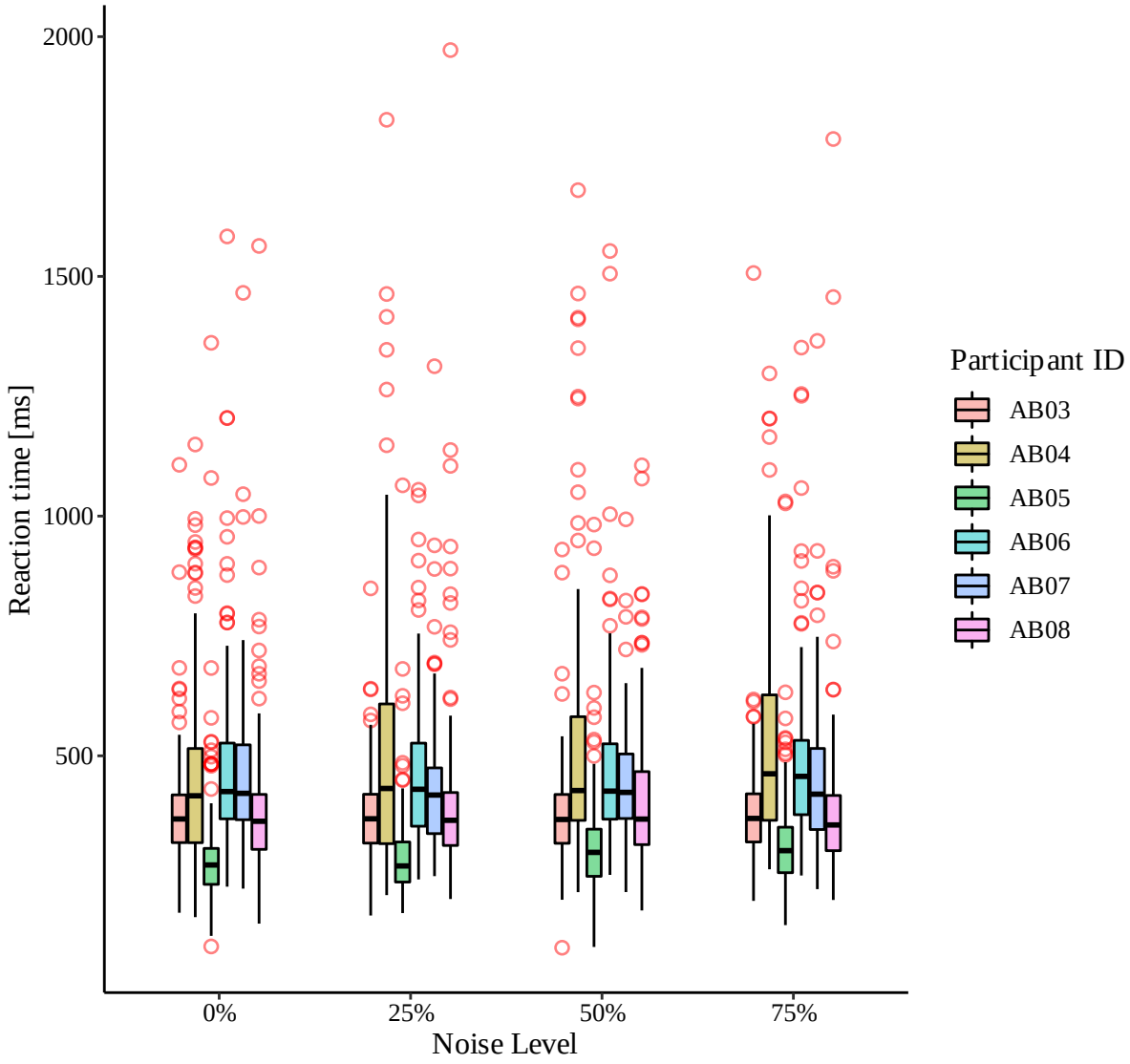

Figure 22. A boxplot showing each participant's reaction times to a red flash on a VR arm, grouped by the concurrent noise level assigned to the VR arm at the time of exposure to the red flash.

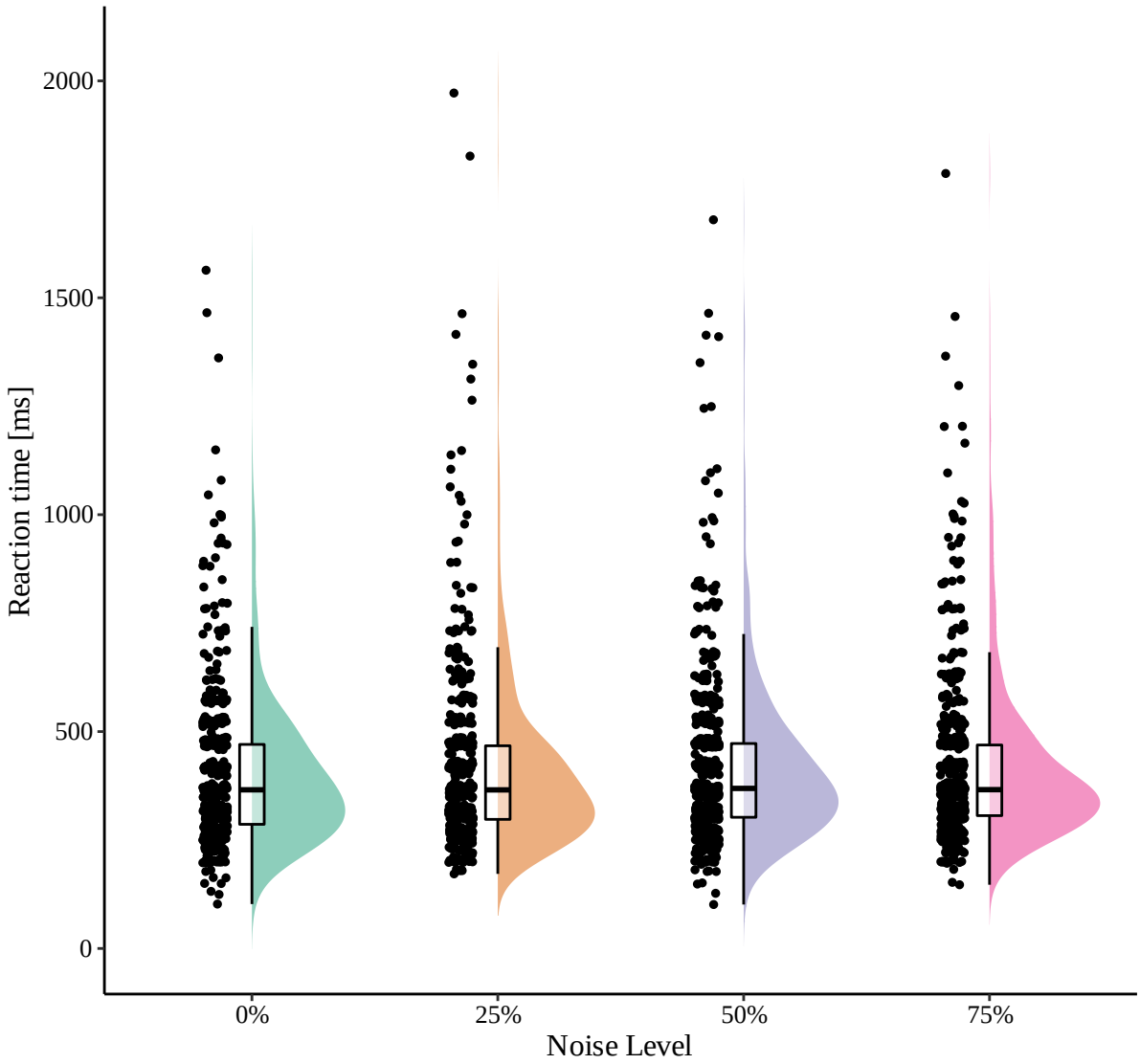

Figure 23. Raincloud plots depicting reaction times to a VR arm flashing red for 200ms, grouped by the concurrent noise level assigned to the VR arm at the time of exposure to the red flash. As indicated by the results of a Kruskal-Wallis test, no statistically significant difference was detected between the noise level groups.

All reaction times plotted in Figure 23 were grouped according to which noise level was assigned to the VR arm when a red flash was detected or reacted to by a press of a keyboard button. As in the gaze data analysis, the dataset from participant AB03 and AB06 was omitted from the test of statistical significance. A Kruskal-Wallis test for significance on each noise level group distribution, $\chi^2(3) = 6.79$, $p = 0.079$, and $n = 2279$, indicated that it was not possible to reject that the reaction time samples from each noise level group came from the same distribution. The results revealed no significant difference between the duration of the reaction time to a VR arm flashing red, no matter the degree of concurrent controllability, thereby, informing the decision to exclude any additional reaction time analysis.

5 Discussion

As previously mentioned, the thesis set out to assess the feasibility of utilizing eye-tracking as an objective measurement of the experience of agency towards a state-of-the-art prosthesis controller based on the pattern recognition of myoelectric signals. With prior research on the sense of agency in mind, an experiment was developed which allowed for MPR-based control over a visual stimulus on a screen, while gaze behavior and reaction time to a simple detection task were recorded. The results obtained from six non-disabled participants suggested that significantly more time was spent fixating on the most controllable virtual arm at any given time. Contrary to the predicted outcome, concurrent controllability over a VR arm did not appear to influence the reaction time to a VR arm flashing red.

In the upcoming sections, the results from the trials will be summarized. Moreover, in light of the exploratory nature of the thesis, some of its drawbacks will be highlighted and suggested future improvements to the study will be discussed.

5.1 Eye-tracking analysis

The results suggested that the overall location of fixation duration varied strongly between participants. Notably, as indicated by the recorded data, a center focused gaze was demonstrated by at least two participants, where the visual attention was primarily oriented to the center area of the visual stimulus, as seen in Figure 16 and Figure 17. This strategy was adopted by AB03, coupled with periodic shifts of gaze to each screen quadrant throughout the trials. These saccadic movements from the center position were most likely attributed to the detection of red flashes on the VR arms, resulting in a rather evenly distributed total fixation duration across AOI encapsulating VR arm of every assigned noise level. The number of red flashes appearing on the VR arms was balanced across each noise level which might also have contributed to the formation of this type of gaze pattern, periodically capturing attention at each noise level.

Each participant's degree of willingness to engage in the experimental task and to maintain compliant towards the instructions throughout the entire duration of the experiment might have been an additional contributory factor in the resulting gaze patterns. The repetitive and lengthy experimental session posed a risk of respondent fatigue setting in, given that prior to the 50 minutes long experiment (excluding breaks between trials), approximately two hours were devoted to briefing and equipment set-up. The reliance of the experimental design on the mental and physical state of the participant, i.e., alertness or patience, possibly influenced their

motivation due to the lengthy process and, in turn, affected which gaze strategy was implemented during the task completion, e.g., an active investigatory or inactive-like gaze behavior. Additionally, internalization or interpretation of task instructions appeared to correspond with each participant's recorded gaze data. During a post-experimental dialogue, AB03 regarded the task as a competitive game and decided to optimize the view of red flashes by focusing on the screen's center and use the peripheral vision to detect red VR arm flashes, while not paying much attention to any changes to VR arm controllability. By contrast, a center-oriented gaze pattern was coupled with another participant (AB06) reporting fatigue due to the repetitive nature of trials and not as a strategy to view the red flashes. However, a more evenly distributed gaze pattern was linked with AB05 account, the fluctuating degrees of VR arm controllability were noticed, and, as a consequence, the most controllable VR arm was actively searched for, while simultaneously reacting to the red flashes. However, the general propensity to look at the screen center during a visual stimulus viewing in an experimental setting (central fixation bias [60]) might have been present for half of the participants (AB03, AB04 & AB06).

Exposing the participants to more noise level affected VR arms resulted in proportionally less area of the visual stimulus being devoted to the most controllable VR arm in each noise condition (three vs. one VR arm). A higher number of fixations captured on the 'noisy VR arms' could be due to the sheer size that they occupied on the screen relative to the single unaltered VR arm. Nevertheless, it is not self-evident that each participant is prone to divide their attention uniformly across all the screen quadrants in front of them. Instead, the VR arm, which is most congruent with the participant's movement, might attract more attention despite being only one amongst three less controllable VR arms, similar to previous findings [13]. As suggested by the heatmaps in Figure 16 and the total fixation duration time on each quadrant portrayed in Figure 17, the fixation distribution was indeed unevenly spread across each quadrant of the screen. Quite apparently seen from Figure 18, the majority of the participants (AB04, AB05, AB07 & AB08) spent more time fixating on the unaltered VR arm interface across all trials. Within each noise condition, the overall result indicated that the participants spent a substantial amount of time fixating on the single unaltered VR arm (1623 sec) compared to the other three (2082 sec) in the high noise condition, see Figure 20.

Lastly, all pairwise comparisons of fixation durations with respect to the ongoing noise level were significantly different, except for 25% and 50% noise level, as seen in Figure 21. All in all, the gaze data results could suggest that visual attention is preferentially attracted to a VR arm that provides the best agentic experience to the participant.

5.2 Reaction time analysis

Conversely, the reaction time results were not in line with our predicted outcome. The expectation was that the participants would react faster to the change of the VR arm's appearance (200 ms red flash) that was most congruent with the subject's intended movements at any moment due to longer fixation durations devoted to that VR arm. On the contrary, no significant difference was observed in reaction times to red flashes on the VR arm depending on the concurrent noise level assigned, as seen in Figure 23. The findings do not coincide with the results of previous studies where a "Self pop-out" effect has been observed when detecting a visual stimulus reproducing participant's self-generated movements in a self-discrimination task [13], and that attentional capture seems to be affected by predictable consequences of actions [61].

Inter-participant differences in reaction time at each concurrent noise level appeared to be reasonably constant, as seen in Figure 22. Meaning that, per participant, the concurrent noise level of the VR arm did not seem to significantly affect the time taken to respond to a VR arm flashing a red color. Moreover, each participant's gaze-strategy (as mentioned above) might not have influenced the reaction times as expected. Comparing the high-controllability focused gaze-strategy (AB05) with the centralized screen fixation strategy (AB03 & AB06), the reaction times remained relatively unchanged across each noise level. Ultimately, leading to the lack of evidence to support the claim that red flash responses on the most controllable VR arm are faster compared to those occurring on 'noisy' VR arms.

5.3 Limitations

This thesis concentrated on creating and assessing the feasibility of a method in which the experience of agency could be objectively measured towards an MPR-controlled prosthetic limb. In order to achieve that goal, the thesis's scope was limited by various factors as well as the shortcomings that were encountered during the development of the experiment and data gathering. The findings of the experiments should be considered alongside these limitations.

The aim was to contribute to the improvement of prosthetics treatments. Thus, it would have been optimal to recruit a representative sample, i.e., amputees, for which prosthetic solutions are designed. Unfortunately, mainly due to recruitment availability and time constraints, no amputees were recruited, which might have otherwise provided further justification to draw any conclusions outside the context of this project.

Several weaknesses of the experimental design were made apparent while running the experiments. Considering the repetitive task provided to each participant during the trials, setting five minutes as the trial length may have caused fatigue to set in well before finishing each trial. As a result, a lack of involvement on the part of the participants might have occurred and affected the outcome measures. By increasing the number of trials, and then reducing their duration by a considerable amount, might alleviate some of the fatigue experienced by this initial design.

As described in detail in the Methods chapter, a wearable eye-tracker was utilized for recording gaze data. The intended use for this type of instrument is to examine gaze behavior in test environments that aim to reproduce real-life scenarios, involving interaction with physical objects by subjects with the possibility of moving around, e.g., store-shelf studies and unboxing of consumer products. Prioritizing the ecological validity of a study comes at the cost of having more complex data analysis due to all gaze points being mapped on to the coordinate system of the video frames captured by the eye-tracking glasses. Therefore, a considerable amount of time was devoted to analyzing where participants looked during the experiment, requiring either a manual or automatic re-mapping procedure of gaze points onto the coordinate system of a static reference image of the visual stimulus.

Additionally, a less visually engaging MPR-controlled visual stimulus might have been more appropriate to use. Similar to previous studies on SoA [30], [62], abstract shapes could be used, movable in directions mapped onto classified movements (e.g., hand extension moves the shape upwards on the screen). Participants should nonetheless be able to attribute a sense of agency towards this less complex and controllable visual stimulus despite it not representing their intended movements as well as a 3D-model of a limb. Varying the number of on-screen affected and unaffected controllable objects by noise level might reduce the visual stimulus activity and yield different results as well.

Furthermore, the separation between each VR arm on the screen may have been too small, encouraging participants to use their peripheral vision to detect the red flashes on the VR arms instead of actively moving their eyes across the screen quadrants for detection. This design decision might be reflected in the relatively similar reaction times to red flashes across all concurrent noise levels. A centralized gaze-pattern could be avoided by explicitly instructing the participants to refrain from looking at the center of the screen, otherwise, it could prevent the appearance of upcoming red flashes on the VR arms. Moreover, displaying the VR arms on a larger monitor and redesigning the visual stimulus so that each VR arm is placed further away

from the center of the screen might compel participants to move their eyes around each screen quadrant to complete the task.

5.4 Future work

By addressing these limitations, e.g., its small and unrepresentative sample size, the robustness of any future developed iterations on this work might be improved substantially beyond the exploratory attempt made in this thesis.

Firstly, it is advisable to use a randomized selection method of a representative sample for making any inferences about the target population (amputees), instead of exclusively choosing non-disabled participants based on convenience sampling. Two groups of participants, non-disabled and amputees, for comparative reasons might yield informative results as to whether perceived SoA in this experimental context differs between the physical state of the participants.

Opting for a remote eye-tracker instead of a head-mounted type has the potential to accelerate the time spent on equipment set-up, and gaze data processing through direct mapping of the gaze-data onto the coordinate system of the two-dimensional screen-based visual stimulus, thereby reducing any time spent on data re-mapping, see Figure 14. Placing the eye-tracker near the screen might alleviate the data-loss due to the gradual downward pitch of the participant's head (providing the tracker's field of detection is large enough) and battery running out in the middle of a trial. The subject might become less aware of the ongoing eye-tracking measurement as a result of not wearing a relatively obtrusive head-mounted tracker throughout the trials. On the other hand, any future studies examining limb agency using this methodology in a real-life setting, i.e., in which the virtual limb would be exchanged with a real prosthetic limb as a terminal device to the MPR-control interface, would be better suited for using a wearable eye-tracker.

Complementing the eye-tracking measures with other pre-established means of assessing SoA could potentially add to the validity of the proposed objective assessment method by examining their correlation with each other. A potential beneficial addition to the current approach would be to add experiments in which the intentional binding effect is measured, as well as to directly ask the participants about their agentic experience towards the visual stimulus. The intentional binding experiment would serve as an implicit assessment of SoA towards the MPR control interface. In the same vein as the framework developed by Schofield et al. [12], wherein the participants could be instructed to reach a specific position with the

controllable visual stimulus, triggering an audible tone after a variable delay, and then asked to estimate the interval between the timepoint of reaching the goal position and the tone onset. In the explicit assessment experiments, the participants could be instructed to control a set of visual stimuli for a brief amount of time and then asked to point out the visual stimulus which was most congruent with their movements. In order to preserve the original intention of eliminating participant's attentional bias towards their controllability when recording eye-movements, these two suggested experiments could take place in sessions following the eye-tracking trials.

Different types of control sites could be included in future studies so that lower-limb and trans-humeral prosthesis SoA assessments can be conducted. The experimental protocols could also be adjusted to provide for more natural simultaneous control instead of individual movement prediction at a time. Other possible additions to the present work could be to implement other types of noise implementations such as sped up or slowed down movements and adding a passive control condition. A situation in which the visual stimulus is being moved without intent, animated by pre-recorded movement commands to represent a passive movement and thereby a total lack of agency towards the visual stimulus.

5.5 Conclusion

In this study, a novel and objective assessment approach for measuring the experience of agency towards an MPR-controlled virtual arm using eye-tracking based measures was designed and examined for feasibility. The resulting data indicates that attentional allocation towards highly controllable virtual limbs differed significantly from others of lower controllability. Contrary to the expected outcome, and despite differences in fixation-time across controllability levels, the reaction time to red-colored flashes occurring on the virtual limbs did not differ between concurrent levels of controllability. Given the exploratory nature of this thesis, the findings should be considered in light of the numerous limitations set by the scope of the project as well as by the challenges encountered during development and data analysis. Therefore, further development of the proposed methods in this project is warranted. The resulting work of this thesis lays the groundwork of an approach that can be improved upon and potentially be used as an assessment procedure of perceived SoA towards different control algorithms driving the state-of-the-art myoelectric prosthetic-limb control systems.

Appendix I

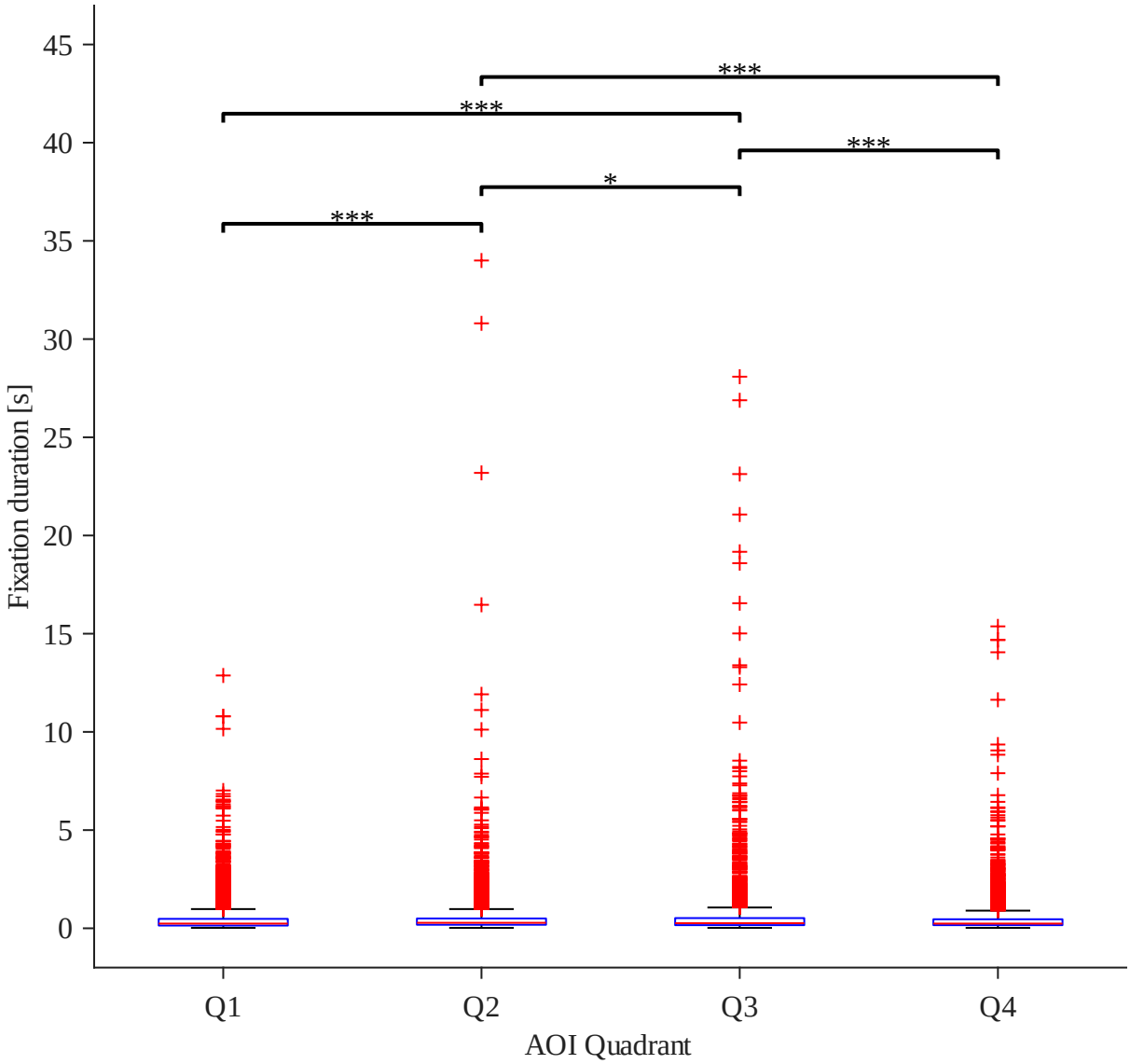

Figure 24. Boxplot showing the eye-fixations durations grouped by AOI screen-quadrant position. Asterisk symbol signifies a statistical difference between fixation duration distributions located on two different AOI screen-quadrants, whereas the absence of asterisk symbols signified the lack of any significant difference between groups.

- A Kruskal-Wallis test indicated that there was a significant difference between some of the eye-fixation duration distributions associated with each AOI, $\chi^2(3) = 108.0649$, $p < 0.0001$. As seen from the pairwise comparisons in Figure 24, the Q2 and Q3 distributions differed significantly from all the other distribution associated with the rest of the quadrants, while only fixations positioned on Q1 and Q4 did not significantly differ.

6 References

[1] P. Gallagher and M. MacLachlan, “Psychological adjustment and coping in adults with prosthetic limbs,” *Behav. Med.*, vol. 25, no. 3, pp. 117–124, 1999.

[2] P. Gallagher, D. Desmond, and M. MacLachlan, *Psychoprosthetics*. Springer Science & Business Media, 2007.

[3] P. L. Ephraim, T. R. Dillingham, M. Sector, L. E. Pezzin, and E. J. MacKenzie, “Epidemiology of limb loss and congenital limb deficiency: A review of the literature,” *Arch. Phys. Med. Rehabil.*, vol. 84, no. 5, p. as0003999303049328, 2003.

[4] G. Rümenapf and S. Morbach, “Editorial : Amputationszahlen - wie sind sie einzuordnen?,” *Dtsch. Arztebl. Int.*, vol. 114, no. 8, pp. 128–129, 2017.

[5] K. Ziegler-Graham, E. J. MacKenzie, P. L. Ephraim, T. G. Travison, and R. Brookmeyer, “Estimating the Prevalence of Limb Loss in the United States: 2005 to 2050,” *Arch. Phys. Med. Rehabil.*, vol. 89, no. 3, pp. 422–429, 2008.

[6] M. Ortiz-catalan, B. Håkansson, and R. Brånemark, “An osseointegrated human-machine gateway for long-term sensory feedback and motor control of artificial limbs,” vol. 6, no. 257, 2014.

[7] E. Mastinu, “Towards clinically viable neuromuscular control of bone-anchored prosthetic arms with sensory feedback,” Chalmers University, 2019.

[8] M. M. D. Sobuh *et al.*, “Visuomotor behaviours when using a myoelectric prosthesis,” *J. Neuroeng. Rehabil.*, vol. 11, no. 1, pp. 1–11, 2014.

[9] J. V. V. Parr, S. J. Vine, N. R. Harrison, and G. Wood, “Examining the Spatiotemporal Disruption to Gaze When Using a Myoelectric Prosthetic Hand,” *J. Mot. Behav.*, vol. 50, no. 4, pp. 416–425, 2018.

[10] Y. Ataria, “Sense of ownership and sense of agency during trauma,” *Phenomenol. Cogn. Sci.*, vol. 14, no. 1, pp. 199–212, 2015.

[11] F. de Vignemont, “Embodiment, ownership and disownership,” vol. 20, pp. 82–93, 2011.

[12] J. S. Schofield, C. E. Shell, Z. C. Thumser, D. T. Beckler, R. Nataraj, and P. D. Marasco, “Characterization of the Sense of Agency over the Actions of Neural-machine Interface-operated Prostheses,” no. January, pp. 1–9, 2019.

[13] R. S. M. L. O. Kannape and J. L. O. Blanke, “‘ Self pop - out ’: agency enhances self - recognition in visual search,” vol. 01, pp. 173–181, 2013.

[14] R. Salomon, S. Szpiro-Grinberg, and D. Lamy, “Self-motion holds a special status in visual processing,” *PLoS One*, vol. 6, no. 10, pp. 2–8, 2011.

[15] P. D. Marasco *et al.*, “Illusory movement perception improves motor control for prosthetic hands,” vol. 10, no. 432, 2018.

[16] S. Gallagher, “Philosophical conceptions of the self : implications for cognitive science,” vol. 4, no. 1, pp. 14–21, 2000.

[17] M. Van Den Bos, E., Jeannerod, “Sense of body and sense of action both contribute to self-recognition,” vol. 85, pp. 177–187, 2002.

[18] R. Groten and M. Slater, “The Sense of Embodiment in Virtual Reality,” vol. 21, no. 4, pp. 373–387, 2012.

[19] N. Braun *et al.*, “The Senses of Agency and Ownership : A Review,” vol. 9, no. April, pp. 1–17, 2018.

[20] N. David, A. Newen, and K. Vogeley, “The ‘sense of agency’ and its underlying cognitive and neural mechanisms,” *Conscious. Cogn.*, vol. 17, no. 2, pp. 523–534, 2008.

[21] J. W. Moore, “What Is the Sense of Agency and Why Does it Matter ?,” vol. 7, no. August, pp. 1–9, 2016.

[22] M. Synofzik, G. Vosgerau, and A. Newen, “Beyond the comparator model: A multifactorial two-step account of agency,” *Conscious. Cogn.*, vol. 17, no. 1, pp. 219–239, 2008.

[23] C. D. Frith, S. J. Blakemore, and D. M. Wolpert, “Abnormalities in the awareness and control of action,” *Philos. Trans. R. Soc. B Biol. Sci.*, vol. 355, no. 1404, pp. 1771–1788, 2000.

[24] J. W. Moore and P. C. Fletcher, “Sense of agency in health and disease: A review of cue integration approaches,” *Conscious. Cogn.*, vol. 21, no. 1, pp. 59–68, 2012.

[25] D. M. Wegner and T. Wheatley, “Apparent mental causation: Sources of the experience of will,” *Am. Psychol.*, vol. 54, no. 7, pp. 480–492, 1999.

[26] W. Wen, A. Yamashita, and H. Asama, “The influence of performance on action-effect integration in sense of agency,” *Conscious. Cogn.*, vol. 53, no. May 2016, pp. 89–98, 2017.

[27] W. Wen, A. Yamashita, and H. Asama, “The sense of agency during continuous action: Performance is more important than action-Feedback association,” *PLoS One*, vol. 10, no. 4, pp. 1–16, 2015.

[28] S. Imaizumi and Y. Tanno, “Intentional binding coincides with explicit sense of agency,” *Conscious. Cogn.*, vol. 67, no. November 2018, pp. 1–15, 2019.

[29] J. A. Dewey, “Do Implicit and Explicit Measures of the Sense of Agency Measure the Same Thing ?,” vol. 9, no. 10, 2014.

[30] F. Argelaguet *et al.*, “The role of interaction in virtual embodiment : Effects of the virtual hand representation To cite this version : HAL Id : hal-01346229 The Role of Interaction in Virtual Embodiment : Effects of the Virtual Hand Representation,” 2016.

[31] J. W. Moore and S. S. Obhi, “Intentional Binding and the Sense of Agency : A review,” pp. 1–39, 2012.

[32] P. Haggard, S. Clark, and J. Kalogeras, “Voluntary action and conscious awareness,” *Nat. Neurosci.*, vol. 5, no. 4, pp. 382–385, 2002.

[33] S. Blakemore, D. M. Wolpert, and C. D. Frith, “Cent ral cancellat ion of self-produced t ickle sensat ion,” pp. 635–640, 1998.

[34] G. Hughes, A. Desantis, and F. Waszak, “Mechanisms of intentional binding and sensory attenuation: The role of temporal prediction, temporal control, identity prediction, and motor prediction,” *Psychol. Bull.*, vol. 139, no. 1, pp. 133–151, 2013.

[35] E. N. Marieb and K. Hoehn, *Human anatomy & physiology*, 12th ed. Pearson Education, 2017.

[36] S. Standring, *Gray’s anatomy: the anatomical basis of clinical practice*, 41st ed. Elsevier Health Sciences, 2015.

[37] P. Geethanjali, “Myoelectric control of prosthetic hands: State-of-the-art review,” *Med. Devices Evid. Res.*, vol. 9, pp. 247–255, 2016.

[38] E. Scheme and K. Englehart, “Electromyogram pattern recognition for control of powered upper-limb prostheses: State of the art and challenges for clinical use,” *J. Rehabil. Res. Dev.*, vol. 48, no. 6, pp. 643–660, 2011.

[39] M. Ortiz-catalan, R. Br, and H. Bo, “BioPatRec : A modular research platform for the control of artificial limbs based on pattern recognition algorithms,” pp. 1–18, 2013.

[40] W. Wen, E. Brann, S. Di Costa, and P. Haggard, “Enhanced perceptual processing of self-generated motion: Evidence from steady-state visual evoked potentials,” *Neuroimage*, vol. 175, pp. 438–448, 2018.

[41] J. M. Wolfe *et al.*, *Sensation & perception*, 3rd ed. Sinauer Sunderland, MA, 2012.

[42] J. V Forrester, A. D. Dick, P. McMenamin, and W. Lee, *The eye*, 4th ed. Elsevier, 2016.

[43] A. T. Duchowski, *Eye tracking methodology: theory and practice*, 3rd ed. Springer, 2017.

[44] A. Bojko, *Eye tracking the user experience: A practical guide to research*. Rosenfeld Media, 2013.

[45] “Activity Stream - Beusable.” [Online]. Available: https://www.beusable.net/features/stream. [Accessed: 10-Dec-2019].

[46] “How do Tobii Eye Trackers work? - Learn more with Tobii Pro.” [Online]. Available: https://www.tobiipro.com/learn-and-support/learn/eye-tracking-essentials/how-do-tobii-eye-trackers-work/. [Accessed: 10-Dec-2019].

[47] “What is Eye Tracking and How Does it Work? - iMotions.” [Online]. Available: https://imotions.com/blog/eye-tracking-work/. [Accessed: 10-Dec-2019].

[48] L. J. Elias, M. P. Bryden, and M. B. Bulman-Fleming, “Footedness is a better predictor than is handedness of emotional lateralization,” *Neuropsychologia*, vol. 36, no. 1, pp. 37–43, Jan. 1998.

[49] “Tobii Pro Glasses 2 wearable eye tracker,” 2015. [Online]. Available: https://www.tobiipro.com/product-listing/tobii-pro-glasses-2/. [Accessed: 06-Sep-2019].

[50] J. Jeff, “Wearable Eye-tracking for Research : comparisons across devices,” 2018.

[51] E. Mastinu, B. Håkansson, and M. Ortiz-catalan, “Low-cost , open source bioelectric signal acquisition system,” pp. 19–22, 2017.

[52] “OGRE - Open Source 3D Graphics Engine | Home of a marvelous rendering engine.” [Online]. Available: https://www.ogre3d.org/. [Accessed: 06-Sep-2019].

[53] D. H. Brainard, “The Psychophysics Toolbox,” *Spat. Vis.*, vol. 10, no. 4, pp. 433–436, 1997.

[54] M. Herlitz, “Analyzing the Tobii Real-world- mapping tool and improving its workflow using Random Forests,” KTH Royal Institute of Technology, 2018.

[55] A. Olsen, “The Tobii I-VT fixation filter,” *Tobii Technology*, 2012. [Online]. Available: https://stemedhub.org/resources/2173/download/Tobii_WhitePaper_TobiiIVTFixationFilter.pdf.

[56] Tobii AB, “Tobii Pro Lab: User’s Manual.” [Online]. Available: https://www.tobiipro.com/siteassets/tobii-pro/user-manuals/Tobii-Pro-Lab-User-Manual/. [Accessed: 27-Sep-2019].

[57] O. V Komogortsev, D. V Gobert, S. Jayarathna, and S. Member, “Standardization of Automated Analyses of Oculomotor Fixation and Saccadic Behaviors,” no. December, 2010.

[58] M. Allen, D. Poggiali, K. Whitaker, T. R. Marshall, and R. Kievit, “Raincloud plots: a multi-platform tool for robust data visualization,” *PeerJ Prepr.*, vol. 6, p. e27137v1, 2018.

[59] A. A. Bojko, “Informative or misleading? Heatmaps deconstructed,” 2009, pp. 30–39.

[60] M. Bindemann, “Scene and screen center bias early eye movements in scene viewing,”

Vision Res., vol. 50, no. 23, pp. 2577–2587, 2010.

[61] N. Kumar, J. A. Manjaly, and M. M. Sunny, “The relationship between action-effect monitoring and attention capture,” *J. Exp. Psychol. Gen.*, vol. 144, no. 1, pp. 18–23, 2015.

[62] W. Wen and P. Haggard, “Control Changes the Way We Look at the World,” *J. Cogn. Neurosci.*, vol. 30, no. 4, pp. 603–619, Apr. 2018.